

Mass wasting and uplift on Crete and Karpathos during the early Pliocene related to initiation of south Aegean left-lateral, strike-slip tectonics

W.J. Zachariasse[†]

Stratigraphy and Paleontology group, Faculty of Geosciences, Utrecht University, Budapestlaan 4, 3584 CD Utrecht, The Netherlands

D.J.J. van Hinsbergen

Paleomagnetic Laboratory "Fort Hoofddijk," Faculty of Geosciences, Utrecht University, Budapestlaan 17, 3584 CD Utrecht, The Netherlands

A.R. Fortuin

Faculty of Earth and Life Sciences, Vrije Universiteit, De Boelelaan 1085, 1081 HV Amsterdam, The Netherlands

ABSTRACT

Reconstruction of the vertical motion history of Crete and Karpathos (southeastern Aegean region, Greece) from the Messinian to Recent revealed a previously poorly documented late Messinian phase of strong subsidence with rates of 50–100 cm/k.y. followed by stasis during the first 250 k.y. of the Pliocene and then by uplift of 500–700 m during the late early to early middle Pliocene. Uplift continued up to Recent albeit at a slower pace and at different rates in different areas. The lower Pliocene in Crete and Karpathos is characterized by widespread occurrences of mass-wasting deposits, which were emplaced over a period of time spanning the first 1.35 m.y. of the Pliocene. The origin of these mass-wasting deposits has long been enigmatic but is here related to uplift which started in Crete as early as ca 5 Ma. It is suggested that the beginning uplift following strong subsidence of various fault blocks until late in the Messinian is related to the onset of south Aegean strike-slip faulting. We postulate that small-scale tilting of fault blocks by trans-tensional strike-slip faulting and increased seismic activity generated slope failures and subsequent sliding of poorly cemented lower Pliocene and uppermost Messinian Lago Mare sediments overlying the terminal Miocene erosional unconformity. The absence of mass-wasting deposits after 3.98 Ma, while uplift continued, is most likely the result of progressive compaction and cementation of the increasingly deeper buried Lago Mare and lower Pliocene sediments, thereby preventing slope failure to a depth of the termi-

nal Miocene unconformity. Hiatuses in some places in Crete and on Karpathos, however, indicate that slope failures continued to occur although on a smaller scale and less frequent than before.

Connecting the change from subsidence to uplift in the earliest Pliocene with the onset of left-lateral, strike-slip tectonics in the south-eastern Aegean arc would make this major strike-slip system much older (by ~2 m.y.) than the generally accepted age of middle to late Pliocene. A recently postulated scenario of "Subduction Transform Edge Propagator" (STEP) faulting to explain the south Aegean strike-slip system predicts rates, distribution, and amount of uplift as rebound to southwestward retreat of the subducted slab along a transform fault zone that is in line with our findings on Crete and Karpathos and explains the absence of compressional structures associated with the uplift, as well as the ongoing southwestward motion of Crete.

Keywords: Crete, vertical motion history, early Pliocene mass wasting, Messinian, geodynamics, Aegean.

INTRODUCTION

The lower Pliocene in Crete and Karpathos (Greece) is unusual in that sediments of this age are in many places represented by unstratified, mass flow deposits of typically several tens of meters thick and made up of ill-sorted mixtures of deep marine, lower Pliocene marls and components of older Neogene strata (up to several meters across) floating in marly matrix. These unusual deposits were first described in some detail from the Ierapetra region by Fortuin (1977), and since then their origin has been

related either to paroxysm (Fortuin, 1978), regional uplift and erosion of the lower Pliocene (Meulenkamp et al., 1979b), submarine sliding due to foundering of fault blocks during the early Pliocene (Peters, 1985), or slope failures during deep submergence at the beginning of the Pliocene of a rejuvenated relief that was shaped during the terminal Miocene (van Hinsbergen and Meulenkamp, 2006). The discussion thus seems to revolve, to a large extent, around the question of whether the emplacement of mass flows followed from uplift during the early Pliocene or from foundering of fault blocks either during early Pliocene or terminal Miocene. Subsidence of the Cretan basins seems to have occurred until at least the latest Miocene (van Hinsbergen and Meulenkamp, 2006). The uplift of Crete was placed in the middle of Pliocene time (Fortuin, 1978; Meulenkamp et al., 1994; van Hinsbergen and Meulenkamp, 2006) with local emergence as early as ca 3.4 Ma (ten Veen and Kleinspehn, 2003), which seems to take the edge off the claim of very early Pliocene uplift. Data on vertical motions during this time span are lacking for Karpathos.

Uncertainties with respect to the origin of the widespread lower Pliocene mass flows on Crete and Karpathos thus concentrate on two major points. The first one focuses on the age range of the mass flows: are individual mass flows separated in time, and if so, what is their precise age range? Secondly, did early Pliocene basins experience strong subsidence or uplift, or stasis, following strong subsidence until and including the Messinian? Solving these issues is a prerequisite to any meaningful discussion that would center on the question of how mass wasting fits in with the vertical motion history of Crete and Karpathos. If mass wasting is causally related to vertical motions, then how did this process

[†]E-mail: jwzach@geo.uu.nl

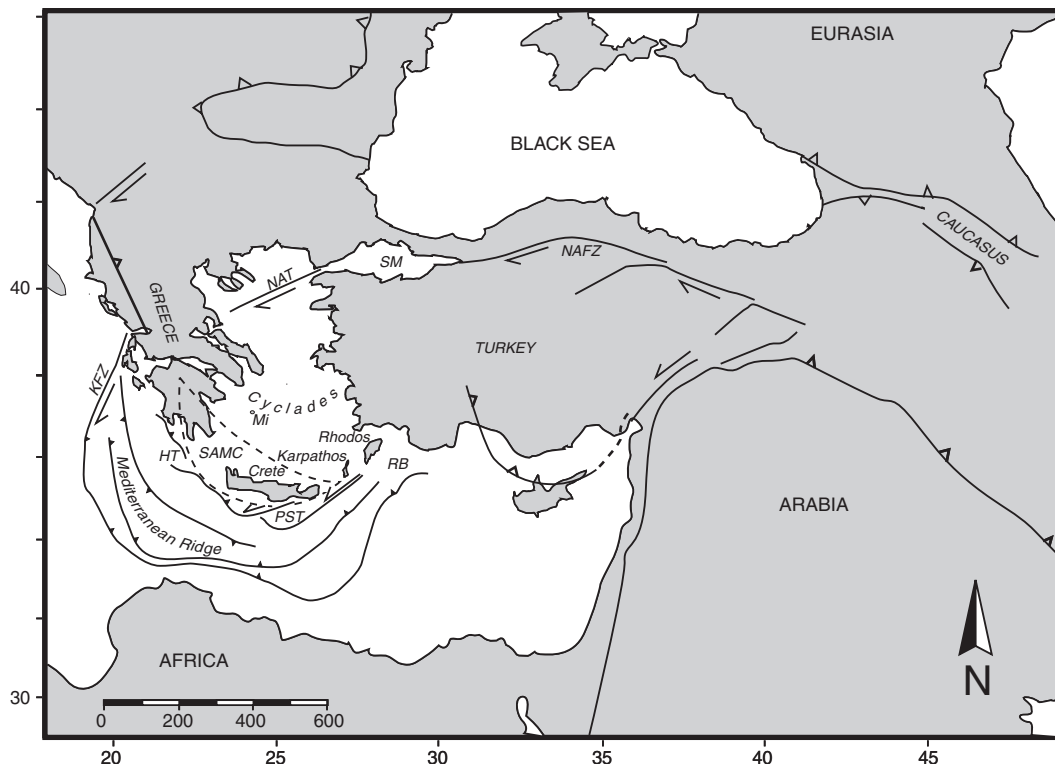


Figure 1. Map of the Aegean region. HT—Hellenic Trench; KFZ—Kefalonia Fault Zone; MI—Milos; NAT—North Aegean Trough; NAFZ—North Anatolian Fault Zone; RB—Rhodes Basin; PST—Pliny and Strabo Trenches; SAMC—Southern Aegean Metamorphic Complex; SM—Sea of Marmara.

come about? And if not, what are the alternatives? In this paper, we present for the first time a detailed description of the lithology, stratigraphic context, and depositional environment of these lower Pliocene mass flows in Crete and Karpathos along with an accurate chronology. Furthermore, we will quantify Messinian to middle Pliocene vertical motions for different areas in Crete and Karpathos by calculating depositional depth values for samples from 38 sections and outcrops spanning the critical time span after correcting for sediment infill and eustasy. It should be noted, however, that a reconstruction of the vertical motion history is greatly hampered by the Messinian Salinity Crisis, which refers to a short period in the history of the Mediterranean (5.96–5.33 Ma; Krijgsman et al., 1999) of massive salt extraction followed by desiccation and refilling during the earliest Pliocene at 5.332 Ma (Lourens et al., 2004). In particular, the removal of a significant portion of the Messinian sediment cover by drawdown-related erosion during the terminal Messinian complicates the reconstruction of vertical motions within the critical time span. An additional problem is that the preserved Messinian sediment cover is often incomplete due to submarine sliding and is not always suitable for meaningful paleobathymetry analysis. Even the lower Pliocene in Crete and Karpathos is rarely complete because of the widespread occurrence of mass-wasting deposits.

GEOLOGIC SETTING

Crete and Karpathos are emerged parts of the Aegean arc located to the north of the Mediterranean Ridge, the surface expression of the accretionary complex, that marks the modern Hellenic subduction zone (Fig. 1). The Aegean arc represents the southern termination of the Aegean lithosphere and has migrated southward several hundreds of kilometers relative to Eurasia since Eocene times as a result of processes including south(west)ward rollback of subducting African lithosphere and associated backarc extension, gravitational collapse, and westward extrusion of Anatolia (Dewey and Şengör, 1979; Le Pichon et al., 1982; Meulenkamp et al., 1988; Jacobshagen, 1994; Fassoulas et al., 1994; Meijer and Wortel, 1997; Cianetti et al., 2001; Jolivet, 2001; Armijo et al., 2004; Kreemer and Chamot-Rooke, 2004). North-south-directed, syn- and post-orogenic extension via low-angle detachments exhumed metamorphic complexes in the Aegean region since the Oligocene (Lister et al., 1984; Gauthier et al., 1993; Ring et al., 2001; Jolivet et al., 2003). On Crete, exhumation of high-pressure/low-temperature (HP/LT) metamorphic rocks occurred between the early Miocene and the late middle to early late Miocene (Fassoulas et al., 1994; Jolivet et al., 1996; Thomson et al., 1998; Rahl et al., 2005). N-S extension via the Cretan detachment was accompanied by the develop-

ment of a large E-W-trending, supra-detachment basin on Crete accommodating the fluvial-lacustrine sediments of the Males river system (van Hinsbergen and Meulenkamp, 2006). This early supra-detachment basin dates back to 12–11 Ma and became increasingly fragmented in the course of the late Miocene by dominantly N-S-striking faults reflecting arc-parallel extension associated with ongoing outward motion of the Aegean arc (ten Veen and Meijer, 1998; Fassoulas, 2001; van Hinsbergen and Meulenkamp, 2006). Finally, some time between the latest Miocene and the late Pliocene, within the same time span as the uplift of Crete, a large system of left-lateral, strike-slip faults including those forming the prominent offshore Pliny and Strabo trenches was formed in the southeastern sector of the Aegean arc. The net result of activity along this fault system is transpression resulting in uplift and counterclockwise rotation in the south Aegean region (Le Pichon et al., 1979; Peters and Huson, 1985; Duermeijer et al., 1998; Mascle et al., 1999; Woodside et al., 2000; ten Veen and Kleinspehn, 2003; van Hinsbergen et al., 2007; Fig. 1).

SECTIONS AND OUTCROPS STUDIED

The lower Pliocene has been studied in 23 locations from all over Crete and in one location on Karpathos (Fig. 2 numbers 1, 3–5, 7, 8b, 8c, 10a, 10b, 11a, 12a, 19–23a, 25a, 25b,

26a, 26b, 27–29, and 31–32). Of these lower Pliocene sections, 17 overlie Miocene rocks, of which 13 expose the contact. Sections 3, 5, 8b, 8c, 10a, 10b, 11b, 12a, 12b, 19–20, 22–23a, 25a, 25b, 26b, 27–29, and 32 are new or re-sampled, whereas sections 1, 4, 7, 11a, 21, 26a, and 31 were subject to earlier studies (see caption Fig. 2), but the samples have been reinvestigated for detailed biostratigraphic and/or paleobathymetric analyses. Sections 2, 6, 9, 14, 15, 16, 24, and 30 refer to Messinian sections and are incorporated in this study solely for paleobathymetry. Of these sections, 2, 14, 15, and 16 are new, whereas sections 6, 9, 24, and 30 are previously published (see caption Fig. 2) but restudied here for biostratigraphy and/or paleobathymetry. Sections 8a, 13, 17, 18, 23b, and 33 are used to portray the timing and magnitude of Pliocene uplift. Section 33 is new, whereas remaining sections were published earlier (see caption Fig. 2), although we improved chronology and extended paleobathymetry analysis for sections 8a, 13, and 18. Additional geographic information on some of the locations is available online in the Appendix (GSA Data Repository)¹.

THE STRATIGRAPHIC RECORD OF THE MESSINIAN AND PLIOCENE

Messinian: The Marine Record

Neogene sediments on Crete are found in a mosaic of faulted basins separated by alpine basement (Fig. 2). This pattern is the result of an intense fragmentation of the large E–W–trending, early supra-detachment basin by successive generations of faults related to a change from dominant N–S to E–W extension in the course of the late Miocene (ten Veen and Postma, 1999b; Fassoulas, 2001). The complex interplay of uplift and erosion and subsidence and infill of the various fault blocks resulted in an extremely complex stratigraphic architecture of the Tortonian infill with considerable vertical and lateral differences in facies and thickness, and cut by numerous hiatuses (see Fig. 7 in van Hinsbergen and Meulenkamp, 2006). Relatively uniform depositional conditions, characterized by deep marine grayish marls, prevailed on Crete at the beginning of the Messinian (van Hinsbergen and Meulenkamp, 2006). At many places, these grayish marls alternate with brownish sapropels reflecting dry-wet climatic conditions paced by the cycle of preces-

sion and modified by obliquity and eccentricity on longer time scales (Hilgen et al., 1995, 1997; Krijgsman et al., 1995). These grayish marine marls with distinct sedimentary cycles belong to the younger part of the Tefeli Group, which is one of the six major lithostratigraphic units distinguished by Meulenkamp et al. (1979a). At several places in central and eastern Crete, these clayey gray marls with intercalated sapropels pass upward either into an alternation of whitish calcareous marls and sapropels, or into calcarenites with occasional calcareous to sapropelitic marls. This unit of whitish calcareous marls and detrital limestones in which low-angle truncations of underlying strata, debris flows, and hiatuses are common is included here in the Vrysses Group, although the boundary with the underlying Tefeli Group is only loosely defined by Meulenkamp et al. (1979a). The lower boundary of the Vrysses Group as defined in this study corresponds with the transition from gray, clayish marls to whitish, highly calcareous marls—a transition often accompanied by input of detrital limestones. Where this transition is sharp, e.g. in locations 9 and 30 (Fig. 2), we were able to date it at 6.72 Ma; elsewhere, in location 16 (Fig. 2), this transition is gradual. On the island of Gavdos, south of Crete, whitish calcareous marls alternating with sapropelitic to diatomaceous beds of the Vrysses Group pass upward into evaporitic limestones marking the level where the so-called Lower Evaporites began to precipitate in the Mediterranean due to a deteriorating connection with the Atlantic (e.g., Meijer, 2006). This level has been dated at 5.96 Ma (Krijgsman et al., 1999). Elsewhere in the Mediterranean these evaporitic limestones pass into gypsum and, in some deep basins, even into halite deposits, but on Gavdos and Crete, in situ deposits of these Lower Evaporites are remarkably rare and incomplete. Except for the evaporitic limestones on Gavdos, in situ Lower Evaporites have been found only near Ploutis (Fig. 2, location 10b) and Tsifout Kastelli (Fig. 2, location 12b) as well as along the road from Agia Varvara to Panasos. At Ploutis, these in situ Lower Evaporites consist almost entirely of alternations of laminated gypsum (“balatino”) and sapropelitic marl, together measuring 50–60 m. At Tsifout Kastelli, they are represented by 20 m of balatino gypsum. In both locations, these Lower Evaporites conformably overlie pre-evaporitic, calcareous, marl-sapropel couplets of the Messinian Vrysses Group. In contrast, they are unconformably overlain by gypsum breccias (see also Fig. 3).

Messinian: The Terrestrial Record

Terrestrial deposits overlying the marine marls, calcarenites, and evaporites of the

Vrysses Group are assigned to the Hellenikon Group (Meulenkamp et al., 1979a). These terrestrial sediments are found at many places in the Mediterranean and mark a short period of some 260 k.y. (5.59–5.33 Ma; Krijgsman et al., 1999) at the end of the Miocene during which the Mediterranean was disconnected from the Atlantic. This period is termed the Lago Mare (sea lake) phase since its introduction (Ruggieri, 1967) and is presently widely accepted to designate the fluvio-lacustrine conditions ending the Messinian prior to the marine Pliocene reflooding. Together with the hyper-saline marine conditions that preceded the Lago Mare phase, these conditions are characteristic of the so-called Mediterranean Messinian Salinity Crisis. The Lago Mare sediments in the area of sections 3 and 4 in western Crete (Fig. 2) are dominated by varicolored (reddish to grayish), coarse clastics along the basin margin and relatively fine-grained clastics away from the margin. This succession is some 250 m thick and deposited in a fluvial to lacustrine environment. Locally, some gypsum beds are intercalated (Meulenkamp et al., 1979b). A field study in 2005 revealed a number of interesting Lago Mare outcrops in the southern part of central Crete at Kourtes (Fig. 2, location 10a), Ploutis (Fig. 2, location 10b), Ano Akria (Fig. 2, location 12a), and nearby Tsifout Kastelli (Fig. 2, location 12b).

The Lago Mare record at Tsifout Kastelli and Ploutis begins with breccias composed of gypsum- and non-fossiliferous limestone clasts (up to 1 m across) floating in a siltitic to arenitic calcareous matrix (measuring some 30–40 m in Tsifout Kastelli and 20 m in Ploutis). Upward, there is a partially exposed alternation of non-fossiliferous clayey, to silty chinks with turbidites, laminated gypsum beds, and fine- to coarse-grained terrigenous clastics measuring some 50 m at Ploutis and 30 m in Tsifout Kastelli (Fig. 3). The many turbidites and occasional findings of gyrogonites of Charaphyta in the chinks and silty clays point to deep lacustrine conditions, whereas the laminated gypsum and terrigenous clastics were most likely deposited in playa lake and fluvial environments. Silty clays relatively rich in foraminifers at Ploutis were sampled in view of claims for occasional flooding of the Mediterranean by Atlantic water during the Lago Mare phase (Carnevale et al., 2006), but foraminifers in these samples are clearly reworked. The Lago Mare sequence at Ploutis and Tsifout Kastelli overlies in situ Lower Evaporites, as described above.

The Lago Mare succession at Ano Akria consists of gypsum breccias overlying pre-evaporitic Messinian calcarenites and sapropels and underlying regularly bedded, lacustrine chinks with interbedded turbidites of at least

¹GSA Data Repository item 2008050, calculated and estimated depth values for all samples along with the relevant faunal data, biozonal assignment or numerical age for all Pliocene samples, and age ranges for Miocene samples, is available at www.geosociety.org/pubs/ft2008.htm. Requests may also be sent to editing@geosociety.org.

20 m thick. Upward, this succession gives way to poorly exposed continental clastics (Fig. 3). Ostracods from Lago Mare deposits at Ano Akria were recently described by Cosentino et al. (2007), but whether their Paratethyan affinity necessarily indicates brackish water conditions remains to be proven.

The Lago Mare succession at Kourtes (Fig. 2, location 10a) is unusual in that it overlies an older stratigraphic unit (Tefeli Group) than the Vrysses Group in the locations mentioned above. Here, two intervals of lacustrine chalks with turbidites alternate with two, respectively 8- and 10-m-thick intervals of continental clastics (Fig. 3). The clasts vary in size from gravel to blocks of 180 cm diameter and consist of both reworked older Neogene and basement rocks, plus a large amount of white, recrystallized, cavernous dolomitic limestones. Similar alternating lacustrine-continental cyclicity is reported from the Nijar Basin (SE Spain), where up to eight continental clastic intervals alternate with lacustrine marly to chalky sediments (Fortuin and Krijgsman, 2003). This type of cyclicity suggests strongly fluctuating lake levels during the Lago Mare phase and, as discussed by Fortuin and Krijgsman (2003), is most likely related to alternating dry-wet climate conditions controlled by the 21-k.y. cycle of precession. Lago Mare deposits in eastern Crete are rare and dominated by continental clastics, although lacustrine cavernous limestones and chalks are occasionally present, for example, to the northwest of location 25 (Fig. 2) at location 386 of Fortuin (1977) and to the northeast of 27 near Ethia (Fig. 2) at the location of Figure 75 in Peters (1985). Lago Mare deposits on Koufonisi are at least 10 m thick and consist of finely bedded azoic calcisiltites to calcarenites with intercalated mass flows dominated by (sub)angular blocks and fragments of azoic porous limestones (see Figs. 13–15 in Peters, 1985). On Karpathos, a 200-m-thick series of fluvio-lacustrine clastics overlies pre-Neogene basement and underlies lower Pliocene mass-wasting deposits (section 32, Figs. 2 and 3). The base of the series consists of 20 m coarse conglomerates with poorly rounded pebbles floating in a mud-matrix and interpreted as a continental mudflow. Higher up, cross-bedded sands are overlain by a travertine bed followed by 100 m silts, sands, and conglomerates with occasionally brackish water ostracods (Daams and Van de Weerd, 1980). A precise age assessment is based on the recovery of an association of small mammals which was first given a Ruscinian (Pliocene; Agustí, 2001) age, but which, according to new insights in eastern Mediterranean mammal biochronology, should have a latest Miocene age (H. de Bruijn, 2006, personal commun.). The fluvio-lacustrine

series on Karpathos thus has been deposited during the Lago Mare phase.

Pliocene

The lowermost Pliocene in Crete and Karpathos consists of deep marine calcareous marls overlying either upper Miocene rocks or basement (sections 1, 3, 4, 7, 10a, 11a, 12a, 18, and 31 in Fig. 3) or lower Pliocene mass-wasting deposits (sections 8b, 8c, 19, 21, 22, 25a, 26a, 26b, 29, and 32 in Fig. 3). These calcareous marls are massive due to intense bioturbation, and steep joints caused blocks to be characteristically rounded by weathering. The CaCO_3 content in these marls is typically 60%–80% (Jonkers, 1984), and only locally, these marls are admixed with clastics (e.g., in locations 4 and 8b). Macrofossils are rare and represented by *Pycnodont* oysters and pectinids. Similar and time-equivalent marls are widespread in the Mediterranean and generally referred to as “Trubi,” which is the name given to this facies on Sicily. Upward, these Trubi marls become less massive and more clayey with numerous brownish sapropelitic or whitish diatomaceous interbeds (Jonkers, 1984). The oldest Pliocene sapropelitic layers in Crete have been found in section 18 (Fig. 3) and have been calibrated (van Hinsbergen and Meulenkamp, 2006) to the prominent northern summer insolation maxima that mark the beginning of a period in which precession values were strongly modulated by the 100 and 400 k.y. eccentricity cycles (5.201–4.912 Ma; Lourens et al., 1996). Cyclically bedded marine sediments extend up into the middle Pliocene in central Crete and the area east of Rethymnon (Zachariasse, 1975), in the area west of Ierapetra (Fortuin, 1977), and on Koufonisi (Dermitzakis and Theodoridis, 1978). The youngest of these middle Pliocene sediments crops out along the south coast of western Crete (at Francocastello; Zachariasse, 1975). At location 13 (Atsipadhes), such cyclically bedded middle Pliocene marly sediments pass upward into bioturbated fine sands (lower part) and sands with irregularly indurated surfaces topped by seven meters of calcareous sands with skeletal debris and large-scale foresets (upper part). The sandy unit measures 90 m and is overlain 3 km to the east by 12 m of poorly exposed sands sometimes with pebbles alternating with calcareous sandstones with transported skeletal debris and pebbles. The sandy unit is middle Pliocene in age (Zachariasse, 1975; van Hinsbergen and Meulenkamp, 2006) and rich in molluscs with admixtures of bryozoans, echinids, and scaphopods. The succession of cyclically bedded marls, via fine sands, to pebbly calcareous sandstones clearly represents a coarsening upward sequence. Together with the rich malacofauna, this succession indicates that

this area rapidly shoaled during the middle Pliocene. The shallow marine sandy unit in the area of locations 12 and 13 and particularly the upper part seems to represent a slightly deeper facies of the fan-delta front deposits described by ten Veen and Kleinspehn (2003) from Agia Galini (west of Timbaki, see Fig. 2). These fan-delta front deposits are made up of bioturbated sands with molluscs and conglomerates showing cross-bedding and have been dated at ca. 3.4 Ma, based on rare occurrences of the planktonic foraminifer *Globorotalia puncticulata* and strontium isotope ratios in foraminifers and molluscs. Although error bars on the Sr-ratios are large and the globorotaliids in the lower shore face sands are certainly reworked (their modern representatives are deep living [Hemleben et al., 1989]), the age of ca. 3.4 Ma agrees well with the middle Pliocene age for the shallow marine sandy unit in the area of locations 12 and 13. The fan-delta front deposits at Agia Galini pass upward and laterally into terrestrial deposits comparable with the terrestrial reddish- to pale-colored cemented conglomerates, sands, and siltstones that conformably overlie the shallow marine sandy unit south of location 12 (but contact is not exposed). These terrestrial clastics are assigned to the Agia Galini Formation (Meulenkamp et al., 1979a) and were given a Pliocene-Pleistocene age on the official geologic map of Greece (Timbakion and Epano Archanæ sheets, 1: 50,000, IGME 1984, 1994). Available age constraints on the underlying, shallow marine clastics at Agia Galini and in the area of locations 12 and 13 indicate that the change-over from shallow marine to terrestrial conditions and the emergence of the southern part of central Crete took place in the middle Pliocene. At two locations—Faneromeni Messara (8a in Fig. 2) and west of Thrapsanon (van Hinsbergen and Meulenkamp, 2006)—the terrestrial clastics of the Agia Galini Formation are found in sharp contact with deep marine lower Pliocene, indicating that both units are separated by an erosional unconformity. If there was a shallowing sequence between the deep marine lower Pliocene and the overlying terrestrial clastics at these locations, then it is removed by subsequent erosion. The distribution area of the terrestrial clastics of the Agia Galini Formation is the southern part of central Crete roughly between Asimi in the east and Timbaki in the west with one small occurrence in the northeastern part of central Crete (Thrapsanon). Nowhere else in Crete do terrestrial clastics conformably overlie middle Pliocene deposits.

LOWER PLIOCENE MASS FLOWS: LITHOLOGY AND AGES

In many places in Crete and Karpathos, basal Pliocene strata consist of chaotic mixtures of

divergent sediment types floating in a marly matrix (sections 5, 8b, 8c, 19–23a, 25–29, and 32 in Fig. 3) and are typically several tens of meters thick. The most common type of mass flow deposits are those in which clasts are dominated by angular blocks (up to several meters across) of cavernous and dense azoic limestones, and lumps of Trubi marls floating in a matrix of homogeneous, or silty marls (Figs. 4A–4C). The lower parts of these mass flow deposits at locations 5, 19, and 27 even incorporate packets of Lago Mare strata that preserve unsorted mass-flow interbeds with abundant angular blocks and fragments of cavernous and dense azoic limestones, which most likely originated from older intra-Lago Mare limestones and/or from the evaporitic limestones of the Vrysses Group (Fig. 4D). The presence of similar limestone clasts floating in the Pliocene mass flows indicates that these clasts are reworked from Lago Mare debris flows. Rare bioclastic limestone fragments (e.g., in locations 19 and 28) are derived from pre-evaporitic limestones of the Vrysses Group. An extreme example of Lago Mare strata incorporated in lower Pliocene mass flow deposits is exposed in location 8b, where large packets of azoic conglomerates and sands are slumped and mixed with contorted packets of Trubi (Fig. 4G). Divergent types of Pliocene mass flow deposits are those dominated by blocks of selenitic gypsum at locations 21 and 22 or even older units of Tortonian age at location 27 underlying the classic type of mass flow deposits (Fig. 3). Biostratigraphic dating of samples taken during a field trip in 2005 from some marly clasts below the main body of gypsum olistoliths in section 22 (Figs. 4E and 4F) confirms the early Pliocene age of this type of mass flow deposits. A similar mass flow deposit with gypsum blocks at location 8c has not been dated but is placed in the lower Pliocene by comparison with the succession at the nearby location 8b (Fig. 3).

The gypsum blocks incorporated in the lower Pliocene mass flow in location 21 and 22 and those in the mass flow tentatively placed in the lower Pliocene at locations 8c may have been reworked from the Lago Mare since gypsum breccias and laminated gypsum beds at Ploutis (Fig. 3) and Tsifout Kastelli (Fig. 3) form part of the Lago Mare succession on Crete and which for their part may be the product of resedimentation of the Lower Evaporites.

Ages of fourteen individual Pliocene mass flows are given in Figure 5. These ages are based on the presence and/or absence of age diagnostic planktonic foraminifers in Trubi clasts and/or from undisturbed Trubi marls directly overlying the mass deposits and the interpretation of these data in terms of six biozones of which the

ages of their defining bioevents are taken from Lourens et al. (2004). Biozone 1 is the interval from base Pliocene (5.332 Ma) to base *Sphaeroidinellopsis subdehiscens* acme (5.30 Ma). On Sicily, in the Global Stratotype Section and Point (GSSP) for the base Pliocene at Eraclea Minoa (van Couvering et al., 2000), biozone 1 contains two smaller intervals with dominant left-coiled neogloboquadrinids (with percentages of >80): one in the upper part of the first precession controlled sedimentary cycle above base Pliocene and the other in the upper and lower part of cycles 2 and 3 (Lourens et al., 1996). In Crete (sections 3, 4, 10a, and 18 in Fig. 3) the double peak has merged into one single maximum due to the more intense bioturbation in the shallower Cretan sections. Biozone 2 defines the interval of the acme of *Sphaeroidinellopsis subdehiscens* (5.30–5.21 Ma). Biozone 3 is the interval between top *Sphaeroidinellopsis* acme and the First Common Occurrence (FCO) of *Globorotalia margaritae* (5.21–5.08 Ma). Biozone 4 is defined by the common occurrence of *Globorotalia margaritae* up to the First Occurrence (FO) of *Globorotalia puncticulata* (5.08–4.52 Ma). Biozone 5 is characterized by the joint presence of *Globorotalia margaritae* and *Globorotalia puncticulata* (4.52–3.98 Ma), and biozone 6 covers the interval from the Last Common Occurrence (LCO) of *Globorotalia margaritae* up to the Last Occurrence (LO) of *Globorotalia puncticulata* (3.98–3.57 Ma). Figure 5 shows several interesting aspects. First, it reveals that gravity sliding occurred over an interval of time spanning the first 1.35 millions of years of the Pliocene Epoch, but the timing differs from place to place even in nearby localities. For example, in location 8b, mass wasting followed shortly after the Pliocene flooding event; however, 1 km to the south (section 8c), gravity sliding occurred 0.25–0.81 m.y. later. Second, ages derived from Trubi clasts and overlying Trubi at the same locality suggest that individual mass-wasting events were relatively short lasting events (Fig. 5: sections 8b, 8c, 19, and 23a). Third, the mass flow deposit on Karpathos incorporates Trubi clasts from different biozones, i.e., biozones 2 and 5. Fourth, the brownish apatite coating on top of the mass flow deposit in location 28 marks 0.68–1.31 m.y. of non-deposition, since the lowermost undisturbed Trubi overlying this surface belongs to biozone 5, whereas the mass flow itself has a biozone 2 age.

TERMINAL MIOCENE EROSION

Lower Pliocene sediments in Crete and Karpathos, which are regular Trubi marls or mass flow deposits, are not always in contact with

Lago Mare sediments but are found to overlie older Miocene units as well. In sections 8b, 8c, 19, 21, 22, 25a, 26, and 29, Pliocene sediments are in contact with pre-evaporitic sediments of the Vrysses Group (Fig. 3). At all these locations, the lowermost Pliocene is characterized by mass flow deposits, and one may argue that these mass flows have eroded the Messinian sediments to a pre-evaporitic level within the Vrysses Group. This would imply that locally the total volume of the Lago Mare and Lower Evaporites has been reworked and incorporated in these lower Pliocene mass flow deposits. In fact, these mass flow deposits are dominated by clasts derived from the Lago Mare. Gypsum clasts are notably rare. Gypsum clasts in mass flow deposits of proven early Pliocene age are known only from section 22 (Fig. 3). The mass flow deposits in location 27 (containing one block of gypsum within a chaotic mass of several types of Tortonian marls), 21 (dominated by gypsum clasts), and 8c (lower mass flow is dominated by gypsum clasts) are tentatively placed in the Pliocene, but a terminal Miocene age cannot be excluded since Trubi clasts were not found. All other Pliocene mass flow deposits are completely devoid of gypsum clasts despite the fact that pre-evaporitic sediments underlying the mass flows in sections 8b, 19, 26, and 29 are deep marine and (in case of section 8b) outcrops of in situ Lower Evaporites are found in the same region at location 10b. All these observations seem to indicate that most of the Lower Evaporites in Crete have disappeared before the refilling of the Mediterranean at the beginning of the Pliocene. This viewpoint is substantiated by section 10a (Fig. 3), where a Lago Mare sequence of some 12 m thick made up of lacustrine chalks with turbidites and continental clastics overlies four meters of gray clays, which, based on field evidence, should belong to an older (Tortonian) part of the Tefeli Group. Washed residues from samples taken from these clays turned out to be devoid of calcareous microfossils. The presence of many fish bones and marine algae (pachysphaeriids) and occasionally of arenaceous benthic foraminifers (*Textularia*) and the pyritized infilling of planktonic foraminifers (*Orbulina*) indicate that these clays were originally foraminiferal-rich marls but were decalcified by pedogenesis in dry periods during the Lago Mare phase after erosion has taken away the whole of the Vrysses Group (while ≥ 100 m is preserved only a few kilometers eastward near Agia Varvara). Also at Kandila (location 11a), the Vrysses Group has been completely removed by erosion during the terminal Miocene. Here, shallow marine calcarenites with intercalations of ungraded fine sands of Tortonian age, are overlain by deep marine

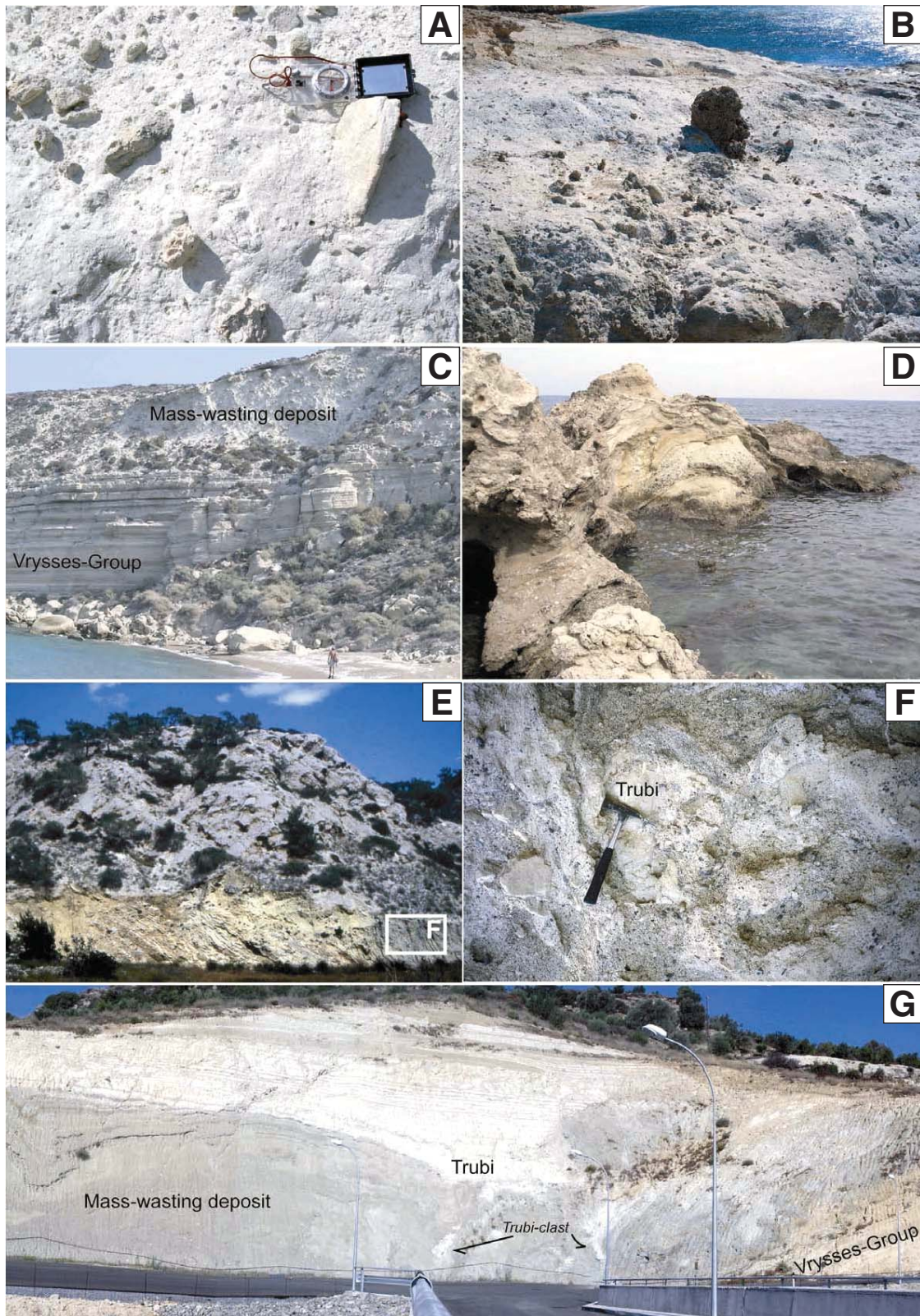


Figure 4. Photographs of lower Pliocene mass-wasting deposits. (A) Prassas, location 19; (B) Punta Beach on Karpathos, location 32; (C) lower Pliocene mass flow overlying deep marine, Messinian calcarenites of the Vrysses Group on Koufonisi, location 30; (D) basal part of lower Pliocene mass flow at Kalyves, location 5, showing contorted packets of Lago Mare sediments; (E) Tertsia, location 22, containing large blocks of selenitic gypsum; (F) detail of basal part of the mass flow shown in Figure 4E; (G) Faneromeni Messara Dam, location 8b, showing deep marine sediments of the Vrysses Group overlain by a chaotic mixture of gravelly Lago Mare and Trubi topped by regular Pliocene.

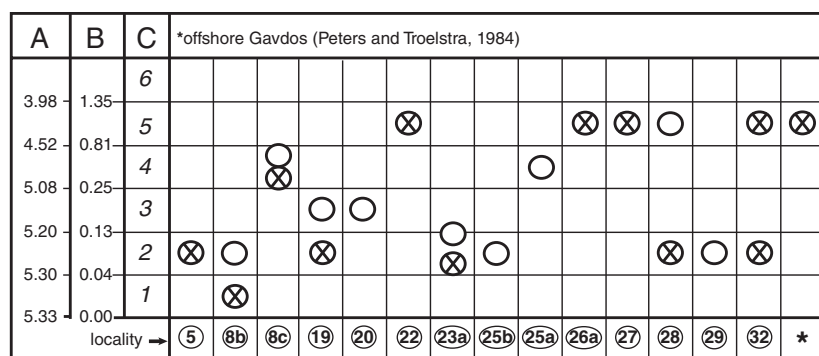


Figure 5. Ages for Trubi clasts in lower Pliocene mass flows (crosses) and (open circles) of undisturbed Trubi directly overlying these mass flows, i.e., contact is exposed. (A) Ages for defining bioevents (from Lourens et al., 2004); and (B) m.y. after Pliocene flooding for successive biozonal boundaries. (C) Planktonic foraminiferal biozones (defined in text). Encircled numbers refer to locations in Figure 2.

Trubi marls. The Tortonian age of these calcarenites could be established in a nearby location (location 11b directly south of Vasiliki along the road to Lendas), where a few meters of marine grayish marls of latest Tortonian age—conformably overlying these calcarenites—escaped erosion during the terminal Miocene (Fig. 3). The irregular and fractured top of the deep marine bioclastic limestones of the Vrysses Group in location 29 suggests karstification after the Lower Evaporites have been cleared away by erosion and dissolution. The gypsum conglomerates found at the base of the Lago Mare sequence in locations 10b and 12b (Fig. 3) also point to erosion and redeposition of a substantial part of the underlying Lower Evaporites. All the observations and conclusions listed above clearly demonstrate that the drawdown related fall in the base level of erosion and subsequent subaerial exposure caused substantial downcutting into underlying units at the beginning or during the early stages of the Lago Mare phase when closure of the Atlantic gateway transformed the Mediterranean into a series of fluvial-lacustrine basins well below mean sea level. Evidence for drawdown-related erosion at the end of the Miocene has been reported earlier from Crete by Peters (1985) and Delrieu et al. (1993). Lago Mare sediments deposited on top of the erosional unconformity have subsequently been incorporated to a large extent into the lower Pliocene mass-wasting deposits (e.g., at locations 5, 8b, 8c, 19, 21, 22, 26, 29, and 30). The failure plane for the early Pliocene mass wasting therefore seems to correspond with the terminal Miocene erosional unconformity as shown for example in Figures 4C and 4G, where deep marine pre-evaporitic Messinian sediments of the Vrysses Group are overlain by lower Pliocene mass-wasting deposits.

VERTICAL MOTION ANALYSIS

Vertical Motions Late in the Messinian

The onlap of deep marine Trubi onto basement rocks in location 31, or onto a few meters of terrestrial sediments (presumably deposited during the Lago Mare phase) overlying basement in location 7 indicates that these locations were emerged before desiccation of the Mediterranean at 5.59 Ma and became deep marine at the beginning of the Pliocene (van Hinsbergen and Meulenkamp, 2006). Calculated and estimated depth ranges for the Trubi marls—using: (1) the regression of van der Zwaan et al. (1990), which relates the percentage of planktonic foraminifers (compared to the number of epifaunal benthic foraminifers) to water depth; and (2) the depth distribution of selected benthic foraminiferal species given in van Hinsbergen et al. (2005)—indicate that water depth at these locations exceeded 500 m during the early Pliocene (Table 1 and caption for more details on the paleobathymetry analysis). The absence of a sedimentary record of transgression suggests that these locations deepened >500 m during the terminal Miocene unless the Trubi in these locations does not represent the earliest Pliocene. Biostratigraphy reveals that biozones 1–3 are missing in location 7 and removal of these biozones by gravity sliding seems likely in view of the wide-spread occurrence of mass flow deposits in Crete. Deepening rates of 2.2–2.4 m/k.y. for the lower Pliocene on Milos (van Hinsbergen et al., 2004) and the upper Miocene in Gavdos (van Hinsbergen and Meulenkamp, 2006) indicate that a deepening of >500 m at location 7 within the earliest 250 k.y. of the Pliocene (being the time span corresponding with the missing biozones) is possible. Foundering of the

area at location 7 thus took place either during the terminal Miocene and/or during the earliest 250 k.y. of the Pliocene. The Trubi marls overlying basement in location 31 belong to biozones 2 and 3. The absence of biozone 1 is most likely due to the fact that the oldest strata have not been sampled rather than that they are missing. Deepening of the area at location 31 (>750 m) therefore should have occurred during the terminal Miocene. The situation at location 32 on Karpathos resembles location 7 in that lower Pliocene overlies Lago Mare sediments, which in their turn overlie basement to the southwest of location 32 (Fig. 3). Unlike section 7, the lowermost Pliocene on Karpathos is made up of mass flow deposits, whereas the thickness of the Lago Mare sediments on Karpathos measures 200 m instead of the few meters in section 7. Figure 5 shows that Trubi clasts incorporated in this mass belong either to biozone 5 or biozone 2. A depositional depth of >750 m for the Trubi clasts from biozone 2 (Table 1) indicates that the deepening of this magnitude must have taken place during the terminal Miocene because the time span of 40 k.y. for biozone 1 is simply too short to establish the deep marine conditions we find here. At location 25a, shallow marine sediments made up of calcarenites with (pebbly) sandstone beds and calcisiltites (in upper part) are sandwiched between basement and lower Pliocene mass flow deposit with regular Trubi on top (Fig. 3). Fossils (oysters and [casts of] pelecypods), locally strong bioturbation, and sedimentary structures point to an inner shelf facies (ca. 50 m deep). The succession most likely belongs to a pre-evaporitic part of the Vrysses Group because of the open marine character of these sediments, although the stratigraphic relationship with other Miocene units is unclear. Strontium isotope dating is prevented by the fact that fossils have been affected by partial recrystallization, possibly as a result of terminal Miocene drawdown and karstification. The oldest Trubi on top of the lower Pliocene mass flow at location 25a belongs to biozone 4, but at the nearby location 25b, it belongs to biozone 2. Combining the depositional depth of the pre-evaporitic Messinian at 25a with that for the Trubi at 25b shows that the Mirabello area deepened more than 500 m during the Messinian, presumably after 6.72 Ma (the age for base Vrysses Group).

All four areas discussed above thus deepened 500–1000 m late in Messinian time. Three areas (7, 31, and 32) stood above sea level before 5.59 Ma (beginning of desiccation) and deepened 500–1000 m during the terminal Miocene, although it cannot be completely excluded that the 500 m deepening at location 7 occurred during the earliest 250 k.y. of the Pliocene. The

TABLE 1. LATE MESSINIAN SUBSIDENCE VALUES FOR KARPATHOS AND DIFFERENT AREAS IN CRETE

Locations in Crete and Karpathos (see Figure 2)	Depositional depth (m) of youngest possible marine Messinian		Depositional depth (m) of lowermost Pliocene (Trubi)		Age range	Late Messinian deepening based on overlapping or nearest values in calculated and estimated depth ranges (m)	Idem, using calculated depth ranges (m)		Subsidence (m) [A = accumulated sediment (m)]
	Calculated	Estimated	Calculated	Estimated			Chora Sfakion area	Chora Sfakion area	
7 Chora Sfakion	Above sea level		632-986	500-600	Biozone 4	~ 600	Chora Sfakion area	Chora Sfakion area	Chora Sfakion area
7 Chora Sfakion (a)						Zakros area	Zakros area	Zakros area	> 500 [A = 5]
31 Xerokambos	Above sea level		909-1238	750-830	Biozone 2 to 3	830-900	Zakros area	Zakros area	> 750 [A = 0]
31 Karpathos Punta Beach	Above sea level		816-1220	~750	Biozone 2	750-800	Karpathos	Karpathos	> 950 [A = 200]
32 Karpathos Punta Beach (b)					Pre-evap. Mess.	Mirabello area	Mirabello area	Mirabello area	> 530 [A = ~30]
25a Pachiammos type	Inner shelf (50 m)		549-857	630-750	Biozone 2	580-700	Vrysses area	Vrysses area	> 350 [A = ~50]
25b Pachiammos road (c)			607-923	500-750	Biozone 2	> 300	Not significant	Not significant	Kastelli area
6 Vrysses	74-291	200-750	766-1155	500-750	Biozone 1 to 2	Not significant	Kastelli area	Kastelli area	100 [A = ~100]
5 Kaiyves (b)	314-1088	350-750	820-1238	500-750	Biozone 2	0-70	Not significant	Not significant	Timbaki area
2 Armenochorio	154-852	100-750	871-1238	500-750	Biozone 1	Zaros area	Zaros area	Zaros area	Max 100 [A = ~20]
1 Kaloudiana (a)	260-894	500-750	755-1179	> 750	Biozone 4	0-100	Not significant	Not significant	Zaros area
8b Fan, Messara Dam	330-880	350-750	811-1238	500-830	Biozone 1 to 2	Miamou area	Miamou area	Miamou area	Max 150 [A = ~50]
9 Agios Ioannis	255-830	350-750	633-1008	350-750	Biozone 3 to 4	Not significant	Not significant	Not significant	5 [A = ~5]
10a Kourtes (a)	102-627	350-750	486-826	630-750	Biozone 1 to 2	Asimi area	Asimi area	Asimi area	Max 130 [A = ~50]
11b Vasiliki Messara	106-676	350-750	740-1089	630-750	Biozone 2 to 3	Heraklion area	Heraklion area	Heraklion area	Heraklion area
14 Parathamna					Biozone 3	Not significant	Not significant	Not significant	50 [A = ~50]
12a Ano Akria (a?)					Biozone 5	Arvi area	Arvi area	Arvi area	
15 Prgos					Biozone 5	Not significant	Not significant	Not significant	
16 Agios Miron					Biozone 5	Arvi area	Arvi area	Arvi area	
18 Kalithea (a)					Biozone 5	Not significant	Not significant	Not significant	
19 Prassas (b + c)					Biozone 5	Arvi area	Arvi area	Arvi area	
20 Patsides (c)					Biozone 5	Not significant	Not significant	Not significant	
21 Arvi					Biozone 5	Arvi area	Arvi area	Arvi area	
21 Arvi (c)					Biozone 5	Not significant	Not significant	Not significant	
22 Tertsia (b)					Biozone 5	Arvi area	Arvi area	Arvi area	
24 NW lerapetra					Biozone 5	Arvi area	Arvi area	Arvi area	
23a Mirros (b + c)					Biozone 5	Arvi area	Arvi area	Arvi area	
26a Sikia					Biozone 5	Arvi area	Arvi area	Arvi area	
26a Sikia (b)					Biozone 5	Arvi area	Arvi area	Arvi area	
30 Koufonisi N-coast					Biozone 5	Arvi area	Arvi area	Arvi area	
28 and 29 Koufonisi SE and SW (b)					Biozone 2	Not significant	Not significant	Not significant	

Note: Subsidence values for Karpathos and different areas in Crete during the late Messinian are obtained by adding the amount of accumulated sediment to the difference in calculated and estimated depth at pre- and post-Lago Mare (right hand column). Calculated depth values are minimum values if the % P values in the regression equation of van der Zwaan et al. (1990) are based on all benthic species except the infaunal species and maximum values if % P values are based on all in situ epifaunal species, i.e. excluding the infaunal species and (allochthonous) epiphytes (including the extinct *Bolivina plicatella*), *Elphidium* spp and *Hantzawaia bouiana* (extinct but epifaunal habitat is doubtful; Morigi et al., 2001). Calculated minimum/maximum and estimated depth values for all samples along with the relevant faunal data plus biozonal assignment or numerical age for Pliocene samples and age ranges for Miocene samples is available in the online GSA Data Repository under Appendix. Depth ranges for the lowermost Pliocene are averages of pairs of minimum and maximum values or only minimum values for the oldest Pliocene samples per section ($n \leq 5$ and marked in grey in the online GSA Data Repository under Appendix). Added to these values is a 1 σ confidence interval of 22 for minimum and 11% for maximum depth values. The σ values represent the average of σ values (in %) calculated for the mean minimum and maximum depth in seven lower Pliocene sections with >5 samples each and together covering biozones 1 to 5 (sections 1, 3, 4, 17, 18, 23a, 28-29, 32 in Figures 3 and 6). Depth ranges for the youngest deep marine pre-evaporitic sediments are averages of only pairs of minimum and maximum values for the youngest possible pre-evaporitic samples per section ($1 \leq n \leq 26$). Added to these values is a 1 σ confidence interval of 48% for minimum and 36% for maximum values derived from averaging σ values (%) for mean minimum and maximum depth in four Messinian sections with >11 samples each (sections 9, 15, 16 and 30 in Figures 2 and 5). Depth and age ranges for sections Agios Miron (16) and Agios Ioannis (9) apply for the youngest 11 and 18 sedimentary cycles, respectively. Suffixes a, b, and c refer to (a) undisturbed Trubi overlying upper Miocene rocks or basement, (b) Trubi clasts in mass flows overlying Miocene rocks, and (c) undisturbed Trubi directly overlying Pliocene mass flows.

Mirabello area (25a) was shallow marine presumably until late in the Messinian (before 6.72 Ma) and deepened 500–750 m between 6.72 and 5.33 Ma. To examine if the already deeply submerged parts of Crete remained at the same depth or deepened as well during the Messinian, 11 areas have been selected for which we quantified the depositional depth of the youngest possible pre-evaporitic sediments and that of the oldest possible Pliocene sediments. This is either based on one vertical succession (sections 8b, 21 [pp], and 26a), or on a combination of two or more outcrops in a geographically limited area (combinations of 1 and 2; 5 and 6; 9 and 10a; 11a and 11b; 12a and 14; 15, 16, 18, 19, and 20; 21 and 22 [pp]; 23a and 24; and 28, 29, and 30). All sections are to be found in Figure 3 with the exception of the unpublished marine Messinian sections 2, 14, 15, and 16 in Figure 6 and the published sections 6, 9, 24, and 30 (for references, see Fig. 2). The depositional depth for the marine Messinian sediments is calculated and estimated in the same way as was done for the lower Pliocene albeit that the 1 σ confidence interval for the calculated Messinian values is larger than the 1 σ value for the lower Pliocene values probably due to the more instable environmental conditions in the Messinian and the overall poor and rapidly changing state of preservation of Messinian foraminifers. Depth and age ranges for the youngest possible pre-evaporitic sediments and the oldest possible Pliocene in the 11 selected areas in Crete are given in Table 1. The age ranges of the few Messinian samples in sections 2, 8b, 11b, 21, 24, and 26 correspond to the age range of the biozone(s) to which samples belong based on biostratigraphic correlation to the astrobiochronology in Krijgsman et al. (1995), Hilgen et al. (1995), and, more recently updated in Lourens et al. (2004). Optimum age constraints are obtained for the Messinian samples in sections 6, 9, 14, 15, 16, and 30 by calibrating sedimentary cycles—made up of gray clayey or white calcareous marls and brown sapropelitic or white diatomaceous clays—to corresponding precession minima and northern summer insolation maxima (for sections 9 and 30, see Hilgen et al. [1997]). The age range of the oldest possible Pliocene samples in the 11 selected areas is obtained by correlation to the succession of six biozones in Figure 5 and defined earlier in the text. Table 1 shows that only one out of these 11 areas deepened significantly (>300 m) during the late Messinian (Vrysses area). For all other areas, no significant deepening trend was found indicating that these areas remained deep during the late Messinian to earliest Pliocene. Deepening trends for the late Messinian are converted into subsidence trends by adding the amount

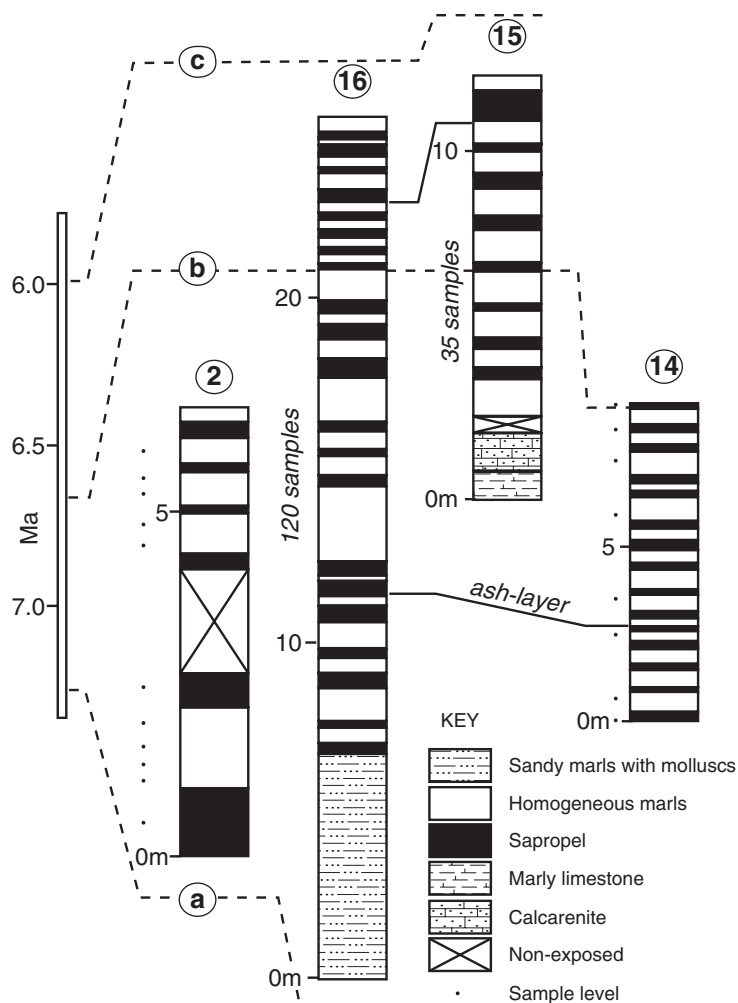


Figure 6. Lithological columns of Messinian sections used for paleobathymetry analysis and not previously published. Numbers refer to locations given in Figure 2. Time markers refer to (A) base Messinian at 7.246 Ma (Lourens et al., 2004), (B) Last Common Occurrence (LCO) of *Globorotalia nicolae* at 6.72 Ma (Lourens et al., 2004), and (C) base of Lower Evaporites at 5.96 Ma (Krijgsman et al., 1999).

of sediments that accumulated during this time span (right-hand column in Table 1). Thickness estimates of upper Messinian sediments in the various areas are based on our field studies and those of Freudenthal (1969) and Meulenkamp et al. (1979b) (Kastelli area); Meulenkamp (1969) and Thomas (1980) (Vrysses area); Fortuin (1977) (Mirabello, Arvi and Ierapetra areas); and Peters (1985) (Sikia area and Koufonisi). The thickness estimates in Table 1 are generally small due to drawdown-related erosion during the terminal Miocene. The assumption we made in converting deepening into subsidence trends is that uplift due to unloading by terminal Miocene erosion is assumed to equal the original subsidence due to sediment loading. Global ice volume change during the late Messinian is negligible (Oerlemans, 2004; van der Laan et al., 2006). The conclusion to be drawn from Table 1 is that

areas that were deep marine at the beginning of Messinian remained at the same depth during the Messinian. Their modest subsidence values (≤ 150 m) reflect net sediment accumulation during the Messinian. An exception is the Vrysses area, which was several hundreds of meters deep late in the Messinian but submerged another 350 m until the beginning of the Pliocene. Several areas that were elevated at the beginning of the Messinian subsided significantly after 6.72 Ma (shallow marine area of Mirabello) and after 5.59 Ma (emerged areas of Chora Sfakion, Zakros and Karpathos) and were deeply submerged at the beginning of the Pliocene.

Vertical Motions during the Pliocene

Paleobathymetric analyses have shown that central Crete shallowed many hundreds

of meters during the early to middle Pliocene (Meulenkamp et al., 1994; van Hinsbergen et al., 2005; van Hinsbergen and Meulenkamp, 2006). The modest thickness of the sediments that accumulated over this time span indicates that most of the shallowing must be attributed to tectonic uplift. Uplift is also nicely exemplified by the lower and middle Pliocene succession in southern central Crete where deep marine Trubi marls pass upward into cyclically bedded more clayey sediments followed by shallow marine sands to calcareous sandstones and topped by terrestrial clastics. To examine whether the early to middle Pliocene uplift trend of central Crete is exemplary for more areas in Crete and for Karpathos and to date the beginning of significant uplift, we analyzed paleobathymetric trends in five composite sections in Crete and Karpathos and compared the results with those of sections 17 and 18 published by van Hinsbergen et al. (2005). Lithological columns of the constituent parts of these composite sections are given in Figure 7. The chronology is based on correlating sections to a succession of ten planktonic foraminiferal biozones, of which the lower six have been defined earlier. Biozone 7 is the interval between LO of *Globorotalia puncticulata* and the FO of *Globorotalia bononiensis* (3.57–3.31 Ma). Biozone 8 defines the interval from the FO of *Globorotalia bononiensis* to base short-term (150 k.y.), absence (low-frequency) interval of this species (3.31–2.87 Ma). Biozone 9 is the short absence interval of *Globorotalia bononiensis* up to the FO of *Neogloboquadrina atlantica* (2.87–2.72 Ma), and biozone 10 defines the interval from the FO of *Neogloboquadrina atlantica* to LO of *Globorotalia bononiensis* (2.72–2.41 Ma). Ages of bioevents are from Lourens et al. (2004). The depth values calculated for the sections in Figure 7 are shown in Figure 8. All calculated depth values (and their averages per biozone) are minimum values except for the Zounaki section (for explanation of calculated minimum and maximum values, see caption Table 1). Benthic foraminiferal depth markers indicate a depositional depth range of 630–750 m at this location at the beginning of the Pliocene (see Appendix [see footnote 1]) so that the high percentages of benthic foraminiferal epiphytes and shallow epifaunal species should have been washed in from the coast. The near coastal setting of the location is inferred from the many intercalations of sands in the lower part possibly representing mouth bars or storm generated beds. Figure 8 shows that the area at locations 12a and 13 shoaled significantly in between biozones 4 and 7. At locations 8a and 8b significant shallowing occurred in between biozones 2 and upper biozone 4, whereas shallowing at locations 23a and 23b took place dur-

ing the time span covered by biozone 4 (Fig. 8). The location of 4 was uniformly deep (~800 m) during the interval of biozones 1 to lower part 4 with slightly deeper conditions recorded for biozone 2. A similar deepening during biozone 2 is observed at location 3 (see Appendix [see footnote 1]). Depth values for Karpathos suggest significant shallowing after biozone 5.

The overall picture that emerges from our paleobathymetry analysis is one of uniformly deep marine conditions during the first 250 k.y. of the Pliocene Epoch (biozones 1–3) followed by significant shallowing of several hundreds of meters during biozone 4 in Crete (5.08 and 4.52 Ma) and later (after 3.98 Ma) in Karpathos. At location 18, significant shoaling seems to have taken place already during biozone 3 but the depth reconstruction here is complicated by the so-called oxygen effect associated with the presence of two sapropels in biozone 3 being the oldest ones recorded in the Pliocene of Crete (for discussion on oxygen effect, see van Hinsbergen et al. [2005]). The magnitude of the shallowing for the composite sections extending up into the middle Pliocene is 800–900 m for sections 12 and 13, and 600–800 m for sections 17 and 18, and ca. 600 m for Karpathos. The lower and middle Pliocene underlying the sandy unit in the area of locations 12a and 13 measures ca. 100 m (based on extrapolating sedimentation rate for section Morias [Zachariasse, 1975] back to base of section 12a), which together with another 100 m for the shallow marine sandy unit and an estimated 50 m for the non-exposed interval between the sandy unit and the terrestrial clastics of the Agia Galini Formation marking regional emergence, totals an uplift of 600–700 m during the late early to early middle Pliocene. Today, the terrestrial clastics in the area of locations 12a and 13 are located at a height of 200–300 m, which, combined with the 50–100 m that has been preserved in this area, would correspond with an uplift of 100–250 m since middle Pliocene time. The composite succession at locations 17 and 18 measures ~100 m and shoaled 600–800 m, pointing to an overall uplift of 500–700 m during the late early to early middle Pliocene. The highest part of the sequence, which today is located at a height of 250–300 m was ~300 m deep at the time of deposition implying a maximum uplift of 500–600 m since the middle Pliocene. This figure can be somewhat refined by subtracting 53 m from the maximum uplift of 500–600 m being the predicted infill until emergence (based on extrapolating shallowing rate to find time of emergence [2.2 Ma] and average sedimentation rate of 5.8 cm/k.y. to calculate infill over interval from middle biozone 8 to 2.2 Ma). Infill after emergence, however, remains unknown. Over-

all uplift of Karpathos during the early and the larger part of the middle Pliocene is ~550 m (i.e., a shoaling of ~600 m during the time span covered by biozones 5 to basal part biozone 10 minus sediment accumulation of ~50 m). The highest part of the sequence, which today is located at 50 m above sea level, was 400 m deep during the upper middle Pliocene. These figures indicate continued uplift of 450 m of Karpathos over the past 2.7 m.y. Adding a correction for infill until emergence of 40 m along the same line as discussed above would result in uplift of ~400 m since the late Pliocene. All evidence together indicates that most of the uplift in the southern Aegean area over the past 5 m.y. took place during the late early to middle Pliocene.

DISCUSSION

Origin of Lower Pliocene Mass-Wasting Deposits

Paleobathymetry analysis of Messinian to lower Pliocene sediments in 15 different areas in Crete and Karpathos has shown that five out of these 15 areas underwent tectonic subsidence of hundreds of meters late in the Messinian. Three of these areas were probably even emerged until 5.59 Ma and subsided more than 500 m during the terminal Miocene (Table 1). All of the 15 areas were 800–1000 m deep at the beginning of the Pliocene and remained that deep during the first 250 k.y. of the Pliocene (being the time span corresponding with biozones 1–3). This period of stasis is followed by uplift during the late early Pliocene and early middle Pliocene, and some of the areas (e.g., southern central Crete) emerged as early as the time interval covered by biozone 8 (3.31–2.87 Ma).

Biostratigraphic analysis of individual mass flows on Crete and Karpathos revealed that the emplacement of these remarkable deposits spans a period of up to 1.35 m.y. following refilling of the Mediterranean with Atlantic water at the beginning of the Pliocene at 5.332 Ma. Eight out of 15 lower Pliocene mass flows were emplaced within the time span corresponding with biozones 1–3, and the remaining seven were deposited within the time interval covered by biozones 4–5. Relating the vertical motion history to the newly established chronology for the lower Pliocene mass flows clearly shows that mass wasting occurred within a period early in the Pliocene in which vertical motions in Crete and Karpathos reversed from subsidence to uplift.

One conclusion may be that mass wasting is not causally related to tectonically induced regional uplift or subsidence but perhaps to refilling of the Mediterranean either through vertical motions as isostatic response to water

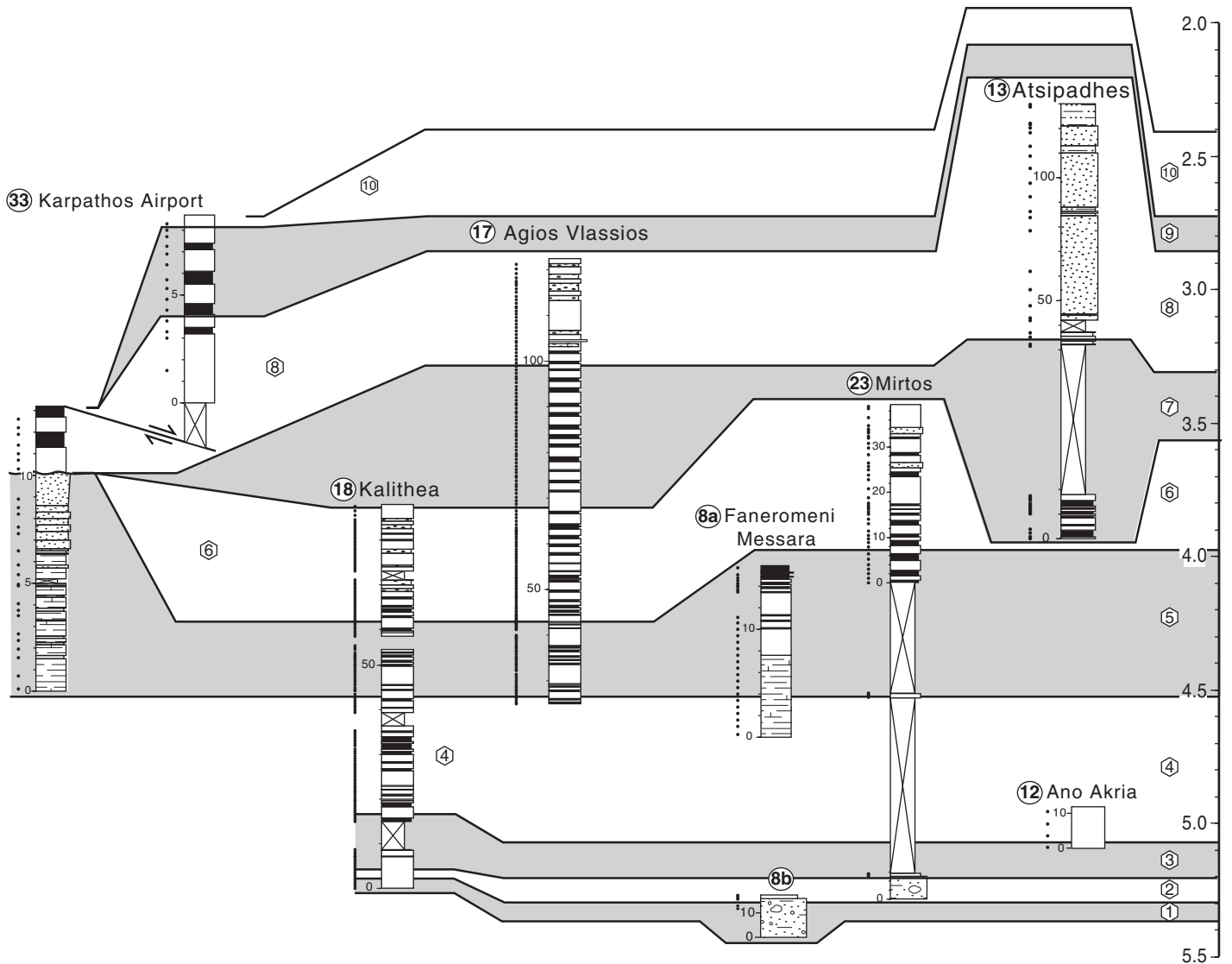


Figure 7. Lithological columns of six composite Pliocene sections used for reconstructing the uplift history of Crete and Karpathos (not plotted along geographic transect for reasons of readability). Encircled numbers and names refer to locations given in Figure 2. Four of the lower Pliocene sections shown in Figure 3 are extended upward by adding younger portion(s) of the succession from the same locality (Kali­theia and Mirtos) or from a nearby location (sections 8a, 8b; 12a–13). The chronology of these Pliocene sections is based on presence and absence patterns of age diagnostic planktonic foraminiferal species and by interpreting these patterns in terms of biozones (numbered 1–10 in hexagons and defined in text). Ages of their defining bioevents are from Lourens et al. (2004).

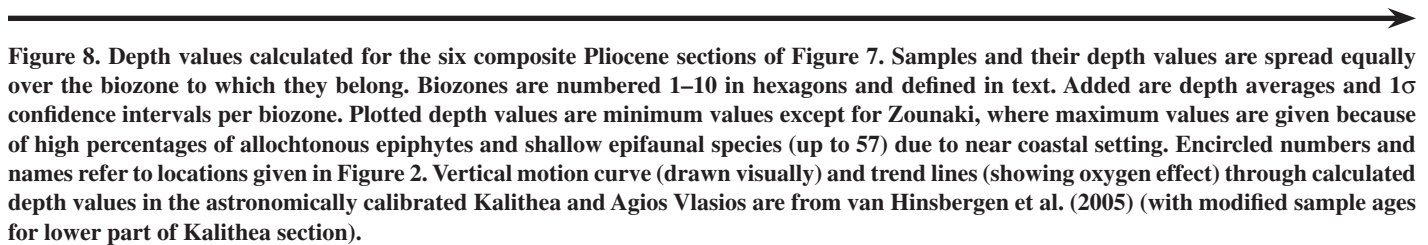
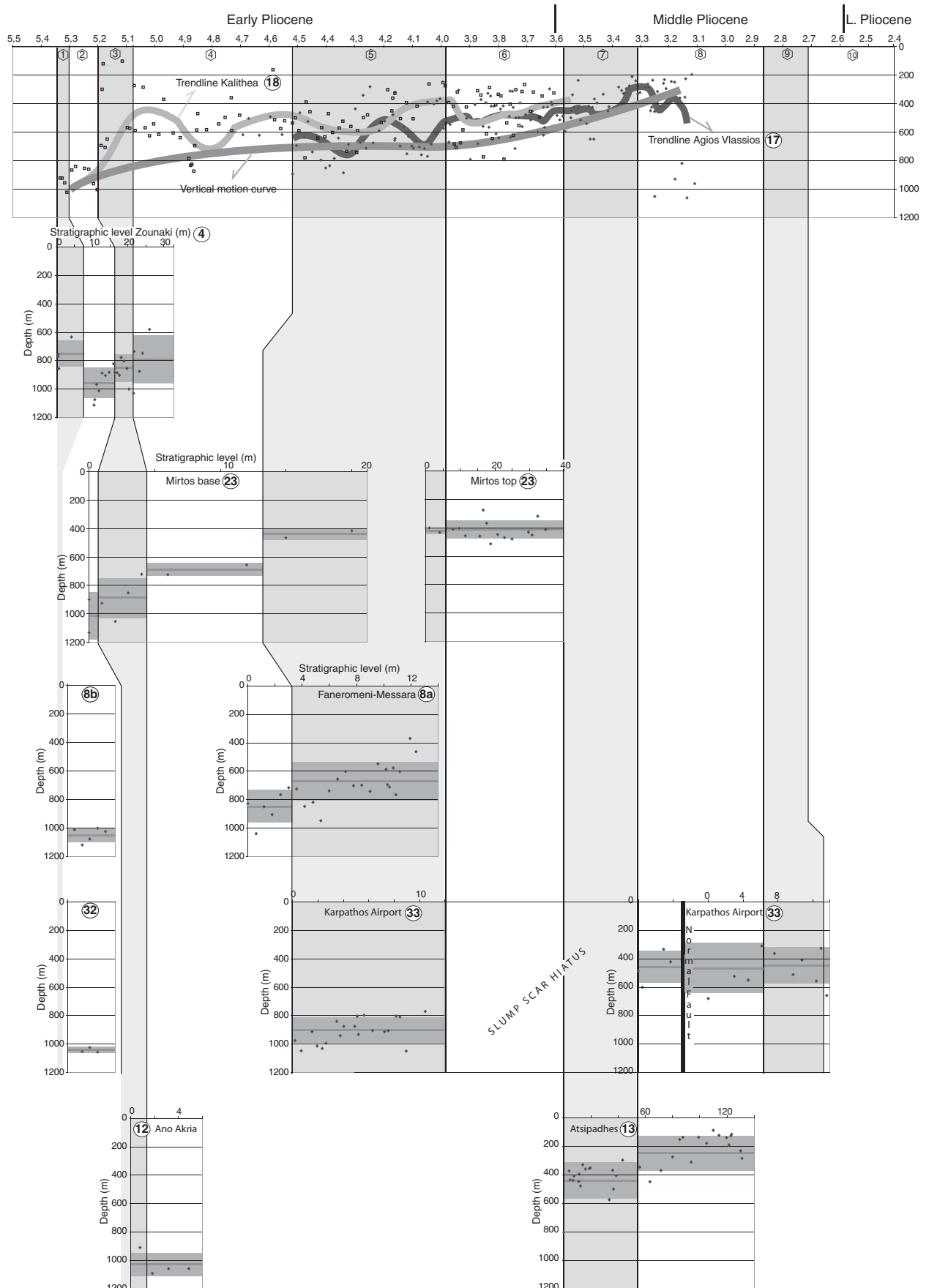


Figure 8. Depth values calculated for the six composite Pliocene sections of Figure 7. Samples and their depth values are spread equally over the biozone to which they belong. Biozones are numbered 1–10 in hexagons and defined in text. Added are depth averages and 1σ confidence intervals per biozone. Plotted depth values are minimum values except for Zounaki, where maximum values are given because of high percentages of allochthonous epiphytes and shallow epifaunal species (up to 57) due to near coastal setting. Encircled numbers and names refer to locations given in Figure 2. Vertical motion curve (drawn visually) and trend lines (showing oxygen effect) through calculated depth values in the astronomically calibrated Kali­theia and Agios Vlassios are from van Hinsbergen et al. (2005) (with modified sample ages for lower part of Kali­theia section).

Late Miocene and Pliocene history of Crete



loading or to drowning of slopes that were covered by debris during the Lago Mare phase. The principle of isostasy predicts that a deep basin that desiccates will react by bouncing upward and by subsiding when the basin is refilled. This principle is nicely exemplified for the Mediterranean in a modeling study by Govers et al. (2007). It shows uplift of deep basins and marginal subsidence once the pre-Lago Mare water load is removed, which reduces the slope angle between margin and deep basin. Conversely, steepening of the slope angle during refilling at the beginning of the Pliocene may have triggered slope instabilities resulting in hiatuses upslope and mass flow deposits downslope. The response time of ~3000 yr of the lithosphere to instantaneous water loading at the beginning of the Pliocene (Govers, 2007, personal commun.), however, is by far too short to consider isostatic adjustment to refilling as the dominant process for the emplacement of mass flows during the first 1.35 m.y. of the Pliocene.

Isostatic response to refilling water as a major driver for early Pliocene mass wasting would also be at odds with the limited geographic distribution of the lower Pliocene mass flows being ubiquitous onshore in Crete and Karpathos with one reported offshore occurrence south of Gavdos (Peters and Troelstra, 1984) and one mass flow deposit drilled at Erosthenes seamount south of Cyprus (Robertson, 1998) of which the age (terminal Miocene or early Pliocene) is unsolved. Similar lower Pliocene mass flows are not found in the Pliocene of Milos and Aegina (van Hinsbergen et al., 2004), the Pliocene of the Ionian Islands (van Hinsbergen et al., 2006), or (to our knowledge) elsewhere in the Mediterranean.

An alternative explanation formulated by van Hinsbergen and Meulenkamp (2006) is that the foundering of various fault blocks in Crete and Karpathos late in the Messinian in combination with talus formation during the Lago Mare phase caused unstable slopes after deep submergence at the beginning of the Pliocene, resulting in slope failures and mass flows. We know now that not all mass flows were emplaced shortly after the Pliocene flooding as assumed by van Hinsbergen and Meulenkamp (2006) but that mass wasting occurred until 1.35 m.y. after the flooding event. Such a large age range seems incompatible with unstable slopes inherited from the terminal Miocene. The long time span and the regional character of mass wasting thus bring us back to the observation that these mass flows were emplaced within a period in which vertical motions in Crete and Karpathos reversed from subsidence to uplift. Even seven out of 15 mass flows were emplaced during an early stage of

significant uplift. Uplift thus began in the earliest 250 k.y. of the Pliocene but became manifest shortly thereafter and continued up to Recent, although rates were largest during the time span bracketed by biozones 4 to and including 8 (5.08–2.87 Ma), when Crete and Karpathos were uplifted by 500–700 m (Fig. 8).

Exploring the possible causal relationship between uplift and mass wasting on Crete and Karpathos invokes several interrelated questions. The first one concerns the origin of uplift. The second one is how uplift initiated long-lasting mass wasting, and the third question then is why this process of mass wasting terminated after 1.35 m.y.

One mechanism explaining the uplift (and exhumation of the HP-LT metamorphosed basement units) of Crete is by subduction-related underplating (e.g., Rahl et al. 2005). However, this process can be inferred to have occurred continuously since the onset of exhumation of the metamorphosed basement units around 21 Ma (Jolivet et al., 1996; Thomson et al., 1998, 1999) and supposedly continues today. There seems no compelling reason to assume that this process increased its influence in terms of uplift between ca. 5 and 3 Ma.

Recently, van Hinsbergen et al. (2007) concluded from rotations and vertical motions on Rhodos, in combination with the absence of Messinian Lower Evaporites in the deep-marine Rhodos basin, which forms the termination of the left-lateral, strike-slip faults forming the Pliny and Strabo trenches (Woodside et al., 2000), that the southern Aegean strike-slip system started to form sometime between 5.3 and 3.8 Ma. This interval corresponds to the period of uplift of Crete, which started around 5 Ma with largest uplift rates shown between 5.08 and 2.87 Ma (the time span bracketed by biozones 4–8). We therefore suggest that the uplift of Crete is related to the formation of the southern Aegean strike-slip system, and that the onset of uplift of Crete around 5 Ma marks the onset of strike-slip deformation. We will discuss the possible relationship between Cretan uplift and onset of the southern Aegean strike slip system below.

It is possible that small-scale tilting of fault blocks and increased seismic activity associated with the initiation of motion along the southern Aegean left-lateral, strike-slip system was sufficient to generate slope failures resulting in hiatuses and mass flows. The slope failure plane—above which poorly consolidated Lago Mare and lower Pliocene sediments slumped down the slope—was most likely the terminal Miocene erosional unconformity. This is particularly evident from three different kinds of observations. First, Lago Mare deposits are missing at all

places (except Karpathos) where we find lower Pliocene mass-wasting deposits (locations 8b, 8c, 19, 21, 22, 25a, 26a, 26b, and 29 in Fig. 3). Second, at several places packets of contorted Lago Mare sediments are incorporated in the basal part of the mass-wasting deposits; and third, on Koufonisi (location 29), we found an erosion remnant of Lago Mare sediments underlain by lower Pliocene mass-wasting deposits. Since we do not find any evidence in the Pliocene for folding or thrusting related to strike-slip tectonics, the magnitude of the tilting must have been modest. Tilting likely occurred along reactivated N100E and N020E normal faults related to arc-parallel stretching and N070E faults related to the initiation of left-lateral, strike slip (Duermeijer et al., 1998; ten Veen and Postma, 1999a, 1999b; Fassoulas, 2001; ten Veen and Kleinspehn, 2003). Mass flows with mixtures of Lago Mare and Trubi clasts were found up into the late early Pliocene corresponding with the early stages of significant uplift, but they are absent in the middle Pliocene (Fig. 5). Submarine sliding, however, did not come to an end since sediments of biozones 6 and 7 are missing in some places in Crete (location 19, [Jonkers, 1984]) and Karpathos (locations 32 and 33, Figure 7 and Appendix [see footnote 1]). We postulate that, as time goes by, continued compaction and cementation of the increasingly deeper buried Lago Mare and Trubi sediments prevented slope failures to a depth of the late Miocene erosional unconformity, thus putting an end to the emplacement of the chaotic mixtures of Trubi and Lago Mare sediments so characteristic for the lower Pliocene in Crete and Karpathos.

Regional Tectonic Implications

Our new, detailed, stratigraphic and vertical motion data and the dating of the lower Pliocene mass-wasting deposits on Crete and Karpathos allow us to quantify the rate, amount, and regional distribution of vertical motions in the south Aegean region. The early stages of activity of the South Aegean left-lateral, strike-slip system were accompanied by regional uplift of 500–700 m of an area several hundreds of kilometers wide, largely between 5 and 3 Ma. Moreover, this Pliocene uplift phase was not accompanied by compressional deformation of Crete or Karpathos. Several scenarios have been proposed explaining this system. It may result from a combination of several geodynamic and kinematic processes in the Aegean region: (1) it may accommodate the westward extrusion of Anatolia into the Aegean region (Dewey and Sengör, 1979); (2) it may have formed as response to increased outward expansion and curvature of the Aegean arc in

combination with collision with the African promontory and the deflection of Aegean arc migration to the southwest (Kissel and Laj, 1988; ten Veen and Kleinspehn, 2003); or (3) it may accommodate the southwestward retreat of the African subducted slab along a “Subduction Transform Edge Propagator,” or STEP fault (Govers and Wortel, 2005). In this paper, we discuss these scenarios within the light of the new quantitative data presented above.

Global positioning system (GPS) measurements and present-day seismicity revealed that westward motion of Anatolia, induced by the collision between Arabia and Eurasia, is currently translated to the Hellenic Trench in the Aegean region along two major strike-slip systems—the left-lateral, south Aegean strike-slip system and the right-lateral, north Aegean strike-slip system, including the Sea of Marmara releasing bend, North-Aegean Trough, and Kefallonia Fault Zone (Hatzfeld, 1999; Kahle et al., 2000; McClusky et al., 2000; Papazachos et al., 2000; Fig. 1). The northern right-lateral, strike-slip system also formed in the latest Miocene to early Pliocene (Armijo et al., 1999; van Hinsbergen et al., 2006), and its generation may therefore indeed be linked to the extrusion of Anatolia. However, superimposed on this motion, the Aegean region itself spreads outward orthogonal to the arc, and this cannot be straightforwardly linked to the extrusion of Anatolia (Meijer and Wortel, 1997; McClusky et al., 2000; Cianetti et al., 2001; Armijo et al., 2004; Flerit et al., 2004; Kreemer and Chamot-Rooke, 2004). The question that now arises is how the uplift of the south Aegean arc is linked with the formation of the south Aegean strike-slip system and whether this could be related to the ongoing outward expansion of the overriding Aegean plate. Here, our new, and recently published (van Hinsbergen and Meulenkamp, 2006) vertical motion information of Crete and Karpathos may provide some answers. A modeling study of Kreemer and Chamot-Rooke (2004) showed that a significant driving source of the Aegean velocity field today is still located south of the Hellenic arc, and southward motion of Crete continues today (McClusky et al., 2000). In addition, it is relevant to note that most of the Pliocene to Pleistocene uplift of Crete took place in the late early to early middle Pliocene despite ongoing southward motion and that the uplift of Crete was not accompanied by compressional deformation. Collision between the African promontory and the southern Aegean margin cannot explain why uplift of Crete and Karpathos seems largely confined to the period between ca. 5 and 3 Ma, why southward motion of Crete continues today, why there is no record of compression accompanying the uplift, and

why the timing and rate of uplift vary from sub-basin to subbasin. An alternative scenario with quantitative predictions for uplift rates, duration, and distribution was recently provided by Govers and Wortel (2005), who explained the formation of the south Aegean strike-slip system and the Kefallonia Fault Zone as STEP faults, along which the subducted African slab rolls back toward the southwest. This scenario includes the formation of isostatically uplifted bulges at the leading edge of the STEP fault. The size, amount, and rate of uplift of these bulges are dependent on the model parameters including rheology and thickness of the lithosphere but are of the same order of magnitude as the dimensions and rates of uplift we reconstructed for Crete. Moreover, this scenario is in line with a driving source south of the Hellenic arc for the Aegean crustal velocity structure: southward expansion and arc-parallel extension continue providing a component of subsidence that may vary in rate and timing from subbasin to subbasin but is superimposed by isostatic uplift, in line with our detailed vertical motion records. We therefore conclude that the STEP-scenario of Govers and Wortel (2005), not excluding the influence of Anatolian extrusion, provides a credible explanation for the formation of the south Aegean strike-slip system and the contemporaneous uplift of Crete due to isostatic rebound.

CONCLUSIONS

Calculated differences in depositional depth between pre-evaporitic Messinian and lowermost Pliocene sediments corrected for sediment infill reveal that various areas in Crete and Karpathos subsided 500–1000 m late in the Messinian. Other areas that were deep marine before the late Messinian remained deep marine during the late Messinian. This late Messinian phase of subsidence fits within ongoing subsidence of different fault blocks throughout the late Miocene related to the expansion of the Aegean arc. All of the studied areas were 800–1000 m deep at the beginning of the Pliocene and remained that deep during the following 250 k.y. Substantial uplift of up to 500–700 m in Crete and Karpathos has been calculated for the late early to early middle Pliocene (ca. 5–3 Ma) albeit at different rates for different areas. We explain these regional variations by the interplay between ongoing local subsidence due to the expansion of the Aegean arc and by regional uplift.

In many places in Crete and on Karpathos, chaotic mixtures dominated by Trubi and Lago Mare sediments overlie in situ Lago Mare sequences or older stratigraphic units. Biostratigraphic analysis of these mass flow deposits

revealed that individual mass flows are clearly separated in time and are emplaced over a period of time spanning the first 1.35 m.y. of the Pliocene. Widespread mass wasting in Crete and Karpathos thus occurred within a period early in the Pliocene in which vertical motions reversed from subsidence to uplift.

The long time span and the regional character of the mass wasting refute the possibility that early Pliocene mass wasting was related to the refilling of the desiccated Mediterranean either through isostatic adjustment to water loading or to deep submergence of unstable slopes loaded by talus formed during drawdown.

The preferred scenario is to connect early Pliocene mass wasting to the process of uplift in Crete and Karpathos. We showed that significant uplift started as early as ca. 5 Ma, and we contend that this is related to the initiation of motion along left-lateral, strike-slip faults superimposed on continued underplating since ca. 21 Ma. Small-scale tilting of fault blocks and increased seismic activity associated with the beginning activity of left-lateral, strike-slip faulting was probably sufficient to generate slope failures resulting in hiatuses and mass flows. We argued that the slope failure plane for mass wasting was most likely the terminal Miocene erosional unconformity. This unconformity—originating from substantial erosion due to a drawdown-related fall in the base level of erosion and subaerial exposure of sediments deposited before desiccation—at places even separates Tortonian from Lago Mare sediments, thus indicating that the whole marine Messinian sediment cover has been removed. At only a few places in Crete, in situ Lower Evaporites escaped drawdown-related erosion and dissolution.

Mass-wasting deposits were found up into the late early Pliocene. The missing of biozones 6 and 7 in some places in Crete and Karpathos, however, indicates that submarine sliding continued but the climax of mass wasting came to an end after 3.98 Ma. At that time, compaction and cementation of increasingly deeper buried Lago Mare and Trubi sediments may have progressed sufficiently long to prevent slope failures to a depth of the terminal Miocene erosional unconformity.

A recently postulated scenario of STEP faulting to explain the south Aegean strike-slip system predicts rates, distribution, and amount of uplift as rebound to southwestward retreat of the subducted slab along a transform fault zone, which is in line with our findings on Crete and Karpathos and explains the absence of compressional structures associated with the uplift, as well as the ongoing southwestward motion of Crete.

ACKNOWLEDGMENTS

Rinus Wortel and Rob Govers are thanked for discussion. Hans de Bruijn and Tanja Kouwenhoven are thanked for their expert opinion on the age of the mammal faunule of Karpathos and benthic foraminiferal depth markers. Sampling on Karpathos was carried out with Johan Meulenkamp, who also provided some of the samples analyzed in this paper. Geert Ittmann is acknowledged for sample preparation and Wil den Hartog for audiovisual assistance. We thank Charalampos Fassoulas, Frank J. Pazzaglia, and an anonymous reviewer for their thorough reviews. This research was conducted within the context of the Netherlands Research School of Integrated Solid Earth Sciences (ISES). DJJvH was supported by a Netherlands Organization for Scientific Research (NOW) VENI grant.

REFERENCES CITED

- Agustí, J., 2001, A calibrated mammal scale for the Neogene of western Europe: State of the art: *Earth-Science Reviews*, v. 52, no. 4, p. 247–260, doi: 10.1016/S0012-8525(00)00025-8.
- Armijo, R., Meyer, B., Hubert, A., and Barka, A., 1999, Westward propagation of the North Anatolian fault into the northern Aegean: Timing and kinematics: *Geology*, v. 27, no. 3, p. 267–270, doi: 10.1130/0091-7613(1999)027<0267:WPOTNA>2.3.CO;2.
- Armijo, R., Flerit, F., King, G., and Meyer, B., 2004, Linear elastic fracture mechanics explains the past and present evolution of the Aegean: *Earth and Planetary Science Letters*, v. 217, no. 1–2, p. 85–95, doi: 10.1016/S0012-821X(03)00590-9.
- Bornovas, I., and Rontogianni-Tsiabaou, T., 1983, Geological map of Greece: Institute of Geology and Mineral Exploration, scale 1:500,000.
- Carnevale, G., Londini, W., and Sarti, G., 2006, Mare versus Lago Mare: Marine fishes and the Mediterranean environment at the end of the Messinian Salinity Crisis: *London, Journal of the Geological Society*, v. 163, no. 1, p. 75–80.
- Cianetti, S., Gasperini, P., Giunchi, C., and Boschi, E., 2001, Numerical modelling of the Aegean-Anatolian region: Geodynamical constraints from observed rheological heterogeneities: *Geophysical Journal International*, v. 146, p. 760–780, doi: 10.1046/j.1365-246X.2001.00492.x.
- Cosentino, D., Gliozzi, E., and Pipponzi, G., 2007, The late Messinian Lago Mare episode in the Mediterranean basin: Preliminary report on the occurrence of Paratethyan ostracod fauna from central Crete, Greece: *Geobios*, v. 40, no. 3, p. 339–349, doi: 10.1016/j.geobios.2007.01.001.
- Daams, R., and Van de Weerd, A., 1980, Early Pliocene small mammals from the Aegean island of Karpathos (Greece) and their palaeogeographic significance: *Geologie en Mijnbouw*, v. 59, no. 4, p. 327–331.
- Delrieu, B., Rouchy, J.-M., and Foucault, A., 1993, La surface d'érosion finimessinienne en Crète centrale (Grèce) et sur le pourtour méditerranéen: Rapports avec la crise de salinité méditerranéenne: *Comptes Rendus Académie Science Paris*, v. 136, no. II, p. 527–533.
- Dermitzakis, M.D., and Theodoridis, S.A., 1978, Planktonic foraminifera and calcareous nannoplankton from the Pliocene of Koufonisi island (East Crete, Greece): *Annuaire Geologique de Pays Hellenique*, v. 29, p. 630–643.
- Dewey, J.F., and Şengör, A.M.C., 1979, Aegean and surrounding regions: Complex multiplate and continuum tectonics in a convergent zone: *Geological Society of America Bulletin*, v. 90, no. 1, p. 84–92, doi: 10.1130/016-7606(1979)90<84:AASRCM>2.0.CO;2.
- Duermeijer, C.E., Krijgsman, W., Langereis, C.G., and ten Veen, J.H., 1998, Post early Messinian counter-clockwise rotations on Crete: Implications for the late Miocene to Recent kinematics of the southern Hellenic Arc: *Tectonophysics*, v. 298, no. 1–3, p. 77–89.
- Fassoulas, C., 2001, The tectonic development of a Neogene basin at the leading edge of the active European margin: The Heraklion basin, Crete, Greece: *Journal of Geodynamics*, v. 31, p. 49–70, doi: 10.1016/S0264-3707(00)00017-X.
- Fassoulas, C., Kiliass, A., and Mountrakis, D., 1994, Post-nappe stacking extension and exhumation of high-pressure/low-temperature rocks in the island of Crete, Greece: *Tectonics*, v. 13, p. 127–138, doi: 10.1029/93TC01955.
- Flerit, F., Armijo, R., King, G., and Meyer, B., 2004, The mechanical interaction between the propagating North Anatolian Fault and the back-arc extension in the Aegean: *Earth and Planetary Science Letters*, v. 224, p. 347–362, doi: 10.1016/j.epsl.2004.05.028.
- Fortuin, A.R., 1977, Stratigraphy and sedimentary history of the Neogene deposits in the Ierapetra region, Eastern Crete: *GUA Papers of Geology*, p. 164.
- Fortuin, A.R., 1978, Late Cenozoic history of eastern Crete and implications for the geology and geodynamics of the southern Aegean region: *Geologie en Mijnbouw*, v. 57, no. 3, p. 451–464.
- Fortuin, A.R., and Krijgsman, W., 2003, The Messinian of the Nijar Basin (SE Spain): Sedimentation, depositional environments and paleogeographic evolution: *Sedimentary Geology*, v. 160, p. 213–242, doi: 10.1016/S0037-0738(02)00377-9.
- Freudenthal, T., 1969, Stratigraphy of the Neogene deposits in the Khania Province, Crete, with special reference to foraminifera of the family planorbiniidae and the genus heterostegina: *Utrecht Micropaleontological Bulletins*, v. 1.
- Gautier, P., Brun, J.-P., and Jolivet, L., 1993, Structure and kinematics of Upper Cenozoic extensional detachment on Naxos and Paros: *Tectonics*, v. 12, p. 1180–1194.
- Govers, R., and Wortel, M.J.R., 2005, Lithosphere tearing at STEP faults: Response to edges of subduction zones: *Earth and Planetary Science Letters*, v. 236, p. 505–523, doi: 10.1016/j.epsl.2005.03.022.
- Govers, R., Meijer, P.Th., and Krijgsman, W., 2007, Solid earth response to Messinian salinity crisis events: *Eos (Transactions, American Geophysical Union)*, v. 87, no. 52, Fall Meeting Supplements, Abstract H13G-07.
- Hatzfeld, D., 1999, The present-day tectonics of the Aegean as deduced from seismicity, *in* Durand, B., Jolivet, L., Horvath, F., and Séranne, M., eds., *The Mediterranean Basins: Tertiary extension within the Alpine orogen*: London, Geological Society of London Special Publication, p. 415–426.
- Hemleben, C., Spindler, M., and Anderson, O.R., 1989, *Modern planktonic foraminifera*: New York, Springer.
- Hilgen, F.J., Krijgsman, W., Langereis, C.G., Lourens, L.J., Santarelli, A., and Zachariasse, W.J., 1995, Extending the astronomical (polarity) time scale into the Miocene: *Earth and Planetary Science Letters*, v. 136, p. 495–510, doi: 10.1016/0012-821X(95)00207-S.
- Hilgen, F.J., Krijgsman, W., and Wijbrans, J.R., 1997, Direct comparison of astronomical and ⁴⁰Ar/³⁹Ar ages of ash beds: Potential implications for the age of mineral dating standards: *Geophysical Research Letters*, v. 24, no. 16, p. 2043–2046, doi: 10.1029/97GL02029.
- IGME, 1984, Geological Map of Greece, Sheet Timbakion: Athens, Institute of Geology and Mineral Exploration (IGME), scale 1: 50,000.
- IGME, 1994, Geological Map of Greece, Sheet Epáno Archanae: Athens, Institute of Geology and Mineral Exploration (IGME), scale 1: 50,000.
- Jacobshagen, V., 1994, Orogenic evolution of the Hellenides: New aspects: *Geologische Rundschau*, v. 83, p. 249–256.
- Jolivet, L., 2001, A comparison of geodetic and finite strain pattern in the Aegean, geodynamic implications: *Earth and Planetary Science Letters*, v. 187, p. 95–104, doi: 10.1016/S0012-821X(01)00277-1.
- Jolivet, L., Goffé, B., Monié, P., Truffert-Luxey, C., Patriat, M., and Bonnaeu, M., 1996, Miocene detachment on Crete and exhumation P-T-t paths of high-pressure metamorphic rocks: *Tectonics*, v. 15, no. 6, p. 1129–1153, doi: 10.1029/96TC01417.
- Jolivet, L., Facenna, C., Goffé, B., Burov, E., and Agard, P., 2003, Subduction tectonics and exhumation of high-pressure metamorphic rocks in the Mediterranean orogen: *American Journal of Science*, v. 303, p. 353–409, doi: 10.2475/ajs.303.5.353.
- Jonkers, H.A., 1984, Pliocene benthonic foraminifera from homogeneous and laminated marls on Crete: *Utrecht Micropaleontological Bulletins*, 179 p.
- Kahle, H.-G., Cocard, M., Peter, Y., Geiger, A., Reilinger, R., Barka, A., and Veis, G., 2000, GPS-derived strain rate within the boundary zones of the Eurasian, African and Arabian Plates: *Journal of Geophysical Research*, v. 105, no. B10, p. 23,353–23,370.
- Kissel, C., and Laj, C., 1988, The tertiary geodynamical evolution of the Aegean arc: A paleomagnetic reconstruction: *Tectonophysics*, v. 146, p. 183–201, doi: 10.1016/0040-1951(88)90090-X.
- Kreemer, C., and Chomot-Rooke, N., 2004, Contemporary kinematics of the southern Aegean and the Mediterranean Ridge: *Geophysical Journal International*, v. 157, p. 1377–1392, doi: 10.1111/j.1365-246X.2004.02270.x.
- Krijgsman, W., Hilgen, F.J., Langereis, C.G., Santarelli, A., and Zachariasse, W.J., 1995, Late Miocene magnetostratigraphy, biostratigraphy and cyclostratigraphy in the Mediterranean: *Earth and Planetary Science Letters*, v. 136, p. 475–494, doi: 10.1016/0012-821X(95)0206-R.
- Krijgsman, W., Hilgen, F.J., Raffi, I., Sierro, F.J., and Wilson, D.S., 1999, Chronology, causes and progression of the Messinian salinity crisis: *Nature*, v. 400, p. 652–655, doi: 10.1038/23231.
- Le Pichon, X., Angelier, J., Aubouin, J., Lyberis, N., Monti, S., Renard, V., Got, H., Hsü, K., Mart, Y., Mascle, J., Matthews, D., Mitropoulos, D., Tsofiias, P., and Chronis, G., 1979, From subduction to transform motion: A seabeam survey of the Hellenic trench system: *Earth and Planetary Science Letters*, v. 44, p. 441–450, doi: 10.1016/0012-821X(79)90082-7.
- Le Pichon, X., Angelier, J., and Sibuet, J.-C., 1982, Plate boundaries and extensional tectonics: *Tectonophysics*, v. 81, p. 239–256, doi: 10.1016/0040-1951(82)90131-7.
- Lister, G., Banga, G., and Feenstra, A., 1984, Metamorphic core complexes of Cordilleran type in the Cyclades, Aegean Sea, Greece: *Geology*, v. 12, p. 221–225, doi: 10.1130/0091-7613(1984)12<221:MCCOCT>2.0.CO;2.
- Lourens, L.J., Antonarakou, A., Hilgen, F.J., Van Hoof, A.A.M., Vergnaud-Grazzini, C., and Zachariasse, W.J., 1996, Evaluation of the Plio-Pleistocene astronomical timescale: *Paleoceanography*, v. 11, no. 4, p. 391–413, doi: 10.1029/96PA01125.
- Lourens, L.J., Hilgen, F.J., Laskar, J., Shackleton, N.J., and Wilson, D., 2004, Chapter 21: The Neogene period, *in* Gradstein, F.M., Ogg, J.G., and Smith, A.G., eds., *A geologic time scale 2004*: Cambridge, Cambridge University Press, p. 409–440.
- Mascle, J., Huguen, C., Benkheilil, J., Chomot-Rooke, N., Chaumillon, E., Foucher, J.P., Griboulard, R., Kopf, A., Lamarche, G., Volkonskaia, A., Woodside, J., and Zitter, T., 1999, Images may show start of European-African plate collision: *Eos (Transactions, American Geophysical Union)*, v. 80, no. 37, p. 421–428, doi: 10.1029/99EO00308.
- McClusky, S., Balassanian, S., Barka, A., Demir, C., Ergintav, S., Georgiev, I., Gurkan, O., Hamburger, M., Hurst, K., Kahle, H., Kastens, K., Kekilidze, G., King, R., Kotzev, V., Lenk, O., Mahmoud, S., Mishin, A., Nadariya, M., Ozounis, A., Paradissis, D., Peter, Y., Prelipin, M., Reilinger, R., Sanli, I., Seeger, H., Tealeb, A., Toköz, M.N., and Veis, G., 2000, Global positioning system constraints on plate kinematics and dynamics in the eastern Mediterranean and Caucasus: *Journal of Geophysical Research*, v. 105, no. B3, p. 5695–5719, doi: 10.1029/1999JB900351.
- Meijer, P.Th., 2006, A box model of the blocked-outflow scenario for the Messinian Salinity Crisis: *Earth and Planetary Science Letters*, v. 248, no. 1–2, p. 486–494, doi: 10.1016/j.epsl.2006.06.013.
- Meijer, P.Th., and Wortel, M.J.R., 1997, Present-day dynamics of the Aegean region: A model analysis of the horizontal pattern of stress and deformation: *Tectonics*, v. 16, no. 6, p. 879–895, doi: 10.1029/97TC02004.
- Meulenkamp, J.E., 1969, Stratigraphy of Neogene deposits in the Rethymnon province, Crete, with special reference to the phylogene of uniserial *Uvigerina* from the

- Mediterranean region: Utrecht Micropaleontological Bulletins, v. 2, p. 168.
- Meulenkamp, J.E., Dermitzakis, M., Georgiadou-Dikeoulia, E., Jonkers, H.A., and Boger, H., 1979a, Field guide to the Neogene of Crete, in Symeonides, N., Papanikolaou, D., and Dermitzakis, M., eds., Publications of the Department of Geology and Paleontology, University of Athens, Series A, No. 32, 32 p.
- Meulenkamp, J.E., Jonkers, H.A., and Spaak, P., 1979b, Late Miocene to Early Pliocene development of Crete: Athens, Proceedings of the Sixth Colloquium on the Geology of the Aegean Region, Athens, v. 1, p. 137–149.
- Meulenkamp, J.E., Wortel, M.J.R., Van Wamel, W.A., Spakman, W., and Hoogerduyn Strating, E., 1988, On the Hellenic subduction zone and the geodynamical evolution of Crete since the late Middle Miocene: Tectonophysics, v. 146, p. 203–215, doi: 10.1016/0040-1951(88)90091-1.
- Meulenkamp, J.E., Van der Zwaan, G.J., and Van Wamel, W.A., 1994, On Late Miocene to Recent vertical motions in the Cretan segment of the Hellenic arc: Tectonophysics, v. 234, p. 53–72, doi: 10.1016/0040-1951(94)90204-6.
- Morigi, C., Jorissen, F.J., Gervais, A., Guichard, S., and Borsetti, A.M., 2001, Benthic foraminiferal faunas in surface sediments off NW Africa: Relationship with organic flux to the ocean floor: Journal of Foraminiferal Research, v. 31, no. 4, p. 350–368, doi: 10.2113/0310350.
- Oerlemans, J., 2004, Correcting the Cenozoic $\delta^{18}\text{O}$ deep-sea temperature record for Antarctic ice volume: Palaeogeography, Palaeoclimatology, Palaeoecology, v. 208, p. 195–205, doi: 10.1016/j.palaeo.2004.03.004.
- Papazachos, B.C., Karakostas, V.G., Papazachos, C.B., and Scordilis, E.M., 2000, The geometry of the Wadati-Benioff zone and lithospheric kinematics in the Hellenic arc: Tectonophysics, v. 319, p. 275–300, doi: 10.1016/S0040-1951(99)00299-1.
- Peters, J.M., 1985, Neogene and Quaternary vertical tectonics in the south Hellenic arc and their effect on concurrent sedimentation processes: GUA papers of Geology, v. 1, no. 23, p. 1–247.
- Peters, J.M., and Huson, W.J., 1985, The Pliny and Strabo trenches (Eastern Mediterranean): Integration of seismic reflection data and SeaBeam bathymetry maps: Marine Geology, v. 64, p. 1–17, doi: 10.1016/0025-3227(85)90157-4.
- Peters, J.M., and Troelstra, S.R., 1984, Early Pliocene sedimentation in the Cretan region: Implications for the timing and amount of vertical motion along the south Hellenic Arc (Eastern Mediterranean): Marine Geology, v. 56, p. 335–344, doi: 10.1016/0025-3227(84)90025-2.
- Rahl, J.M., Anderson, K.M., Brandon, M.T., and Fassoulas, C., 2005, Raman spectroscopic carbonaceous material thermometry of low-grade metamorphic rocks: Calibration and application to tectonic exhumation in Crete, Greece: Earth and Planetary Science Letters, v. 240, no. 339–354.
- Ring, U., Layer, P.W., and Reischmann, T., 2001, Miocene high-pressure metamorphism in the Cyclades and Crete, Aegean Sea, Greece: Evidence for large-magnitude displacement on the Cretan detachment: Geology, v. 29, no. 5, p. 395–398, doi: 10.1130/0091-7613(2001)029<0395:MHPMIT>2.0.CO;2.
- Robertson, A.H.F., 1998, Significance of early Pliocene mass-flow deposits for the timing and process of collision of the Eratosthenes Seamount with the Cyprus active margin in the Eastern Mediterranean (Leg 160), in Robertson, A.H.F., Emeis, K.C., Richter, C., and Camerlenghi, A., Proceedings of the Ocean Drilling Program: Scientific results, 160, p. 465–481.
- Ruggieri, G., 1967, The Miocene and later evolution of the Mediterranean sea, in Adams, C.G., and Ager, D.V., eds., Aspects of Tethyan biogeography: Oxford, UK, Systematics Association Publications, p. 283–290.
- Spaak, P., 1981, The distribution of the Globorotalia inflata group in the Mediterranean Pliocene: Proceeding van de Koninklijke Nederlandse Academie van Wetenschappen: Series B, v. 84, no. 2, p. 201–215.
- ten Veen, J.H., and Kleinspehn, K.L., 2003, Incipient continental collision and plate-boundary curvature: Late Pliocene-Holocene transtensional Hellenic forearc, Crete, Greece: London, Journal of the Geological Society, v. 160, p. 161–181.
- ten Veen, J.H., and Meijer, P.Th., 1998, Late Miocene to Recent tectonic evolution of Crete (Greece): Geological observations and model analysis: Tectonophysics, v. 298, no. 1–3, p. 191–208, doi: 10.1016/S0040-1951(98)00184-X.
- ten Veen, J.H., and Postma, G., 1999a, Neogene tectonics and basin fill patterns in the Hellenic outer-arc (Crete, Greece): Basin Research, v. 11, p. 243–266, doi: 10.1046/j.1365-2117.1999.00098.x.
- ten Veen, J.H., and Postma, G., 1999b, Roll-back controlled vertical movements of outer-arc basins of the Hellenic subduction zone (Crete, Greece): Basin Research, v. 11, p. 223–241, doi: 10.1046/j.1365-2117.1999.00097.x.
- Thomas, E., 1980, Details of Uvigerina development in the Cretan Mio-Pliocene: Utrecht Micropaleontological Bulletins, v. 23, p. 167.
- Thomson, S.N., Stöckert, B., and Brix, M.R., 1998, Thermochronology of the high-pressure metamorphic rocks of Crete, Greece: Implications for the speed of tectonic processes: Geology, v. 26, no. 3, p. 259–262, doi: 10.1130/0091-7613(1998)026<0259:TOTHPM>2.3.CO;2.
- Thomson, S.N., Stöckert, B., and Brix, M.R., 1999, Miocene high-pressure metamorphic rocks of Crete, Greece: Rapid exhumation by buoyant escape, in Ring, U., Brandon, M.T., Lister, G.S., and Willet, S.D., eds., Exhumation processes: Normal faulting, ductile flow and erosion: Geological Society of London Special Publications, p. 87–107.
- van Couvering, J.A., Castradori, D., Cita, M.B., Hilgen, F.J., and Rio, D., 2000, The base of the Zanclean stage and of the Pliocene series: Episodes, v. 23, no. 3, p. 179–186.
- van der Laan, E., Snel, E., de Kaenel, E., Hilgen, F.J., and Krijgsman, W., 2006, No major deglaciation across the Miocene–Pliocene boundary: Integrated stratigraphy and astronomical tuning of the Loulja section (Bou Regreg area, NW Morocco): Paleogeography, v. 21, p. PA3011, doi: 10.1029/2005PA001193.
- van der Zwaan, G.J., Jorissen, F.J., and De Stigter, H.C., 1990, The depth dependency of planktonic/benthonic foraminiferal ratios: Constraints and applications: Marine Geology, v. 95, p. 1–16, doi: 10.1016/0025-3227(90)90016-D.
- van Hinsbergen, D.J.J., and Meulenkamp, J.E., 2006, Neogene supra-detachment basin development on Crete (Greece) during exhumation of the South Aegean core complex: Basin Research, v. 18, p. 103–124, doi: 10.1111/j.1365-2117.2005.00282.x.
- van Hinsbergen, D.J.J., Snel, E., Garstman, S.A., Marunteanu, M., Langereis, C.G., Wortel, M.J.R., and Meulenkamp, J.E., 2004, Vertical motions in the Aegean volcanic arc: Evidence for rapid subsidence preceding in situ volcanism: Marine Geology, v. 209, p. 329–345, doi: 10.1016/j.margeo.2004.06.006.
- van Hinsbergen, D.J.J., Kouwenhoven, T.J., and van der Zwaan, G.J., 2005, Paleobathymetry in the backstripping procedure: Correction for oxygenation effects on depth estimates: Palaeogeography, Palaeoclimatology, Palaeoecology, v. 221, no. 3–4, p. 245–265, doi: 10.1016/j.palaeo.2005.02.013.
- van Hinsbergen, D.J.J., van der Meer, D.G., Zachariasse, W.J., and Meulenkamp, J.E., 2006, Deformation of western Greece during Neogene clockwise rotation and collision with Apulia: International Journal of Earth Sciences, v. 95, no. 3, p. 463–490, doi: 10.1007/s00531-005-0047-5.
- van Hinsbergen, D.J.J., Krijgsman, W., Langereis, C.G., Corné, J.-J., Duermeijer, C.E., and van Vugt, N., 2007, Discrete Plio-Pleistocene phases of tilting and counterclockwise rotation in the southeastern Aegean arc (Rhodos; Greece): Early Pliocene formation of the south Aegean left-lateral strike-slip system: London, Journal of the Geological Society, v. 164, p. 1133–1144.
- Woodside, J., Mascle, J., Huguen, C., and Volkonskaia, A., 2000, The Rhodes basin, a post-Miocene tectonic trough: Marine Geology, v. 165, p. 1–12, doi: 10.1016/S0025-3227(99)00140-1.
- Zachariasse, W.J., 1975, Planktonic foraminiferal biostratigraphy of the Late Neogene of Crete (Greece): Utrecht Micropaleontological Bulletins, v. 11, p. 171.

MANUSCRIPT RECEIVED 2 JANUARY 2007

REVISED MANUSCRIPT RECEIVED 13 SEPTEMBER 2007

MANUSCRIPT ACCEPTED 17 OCTOBER 2007

Printed in the USA